GEOACTA **37**(2): 83-116 (2012) ISSN 1852-7744

NEW DETAILED HOLOCENE PALEOMAGNETIC RECORDS WITH ANOMALOUS GEOMAGNETIC FIELD BEHAVIOR IN ARGENTINA

Hugo G. Nami [1 2]

[1] CONICET-Instituto de Geofísica "Daniel A. Valencio" (INGEODAV), Departamento de Ciencias Geológicas, Facultad de Ciencias Exactas, Físicas y Naturales, Universidad de Buenos Aires, Ciudad Universitaria (Pabellón II), (1428) Buenos Aires, Argentina.
[2] Associated researcher, National Museum of Natural History, Smithsonian Institution, Wa. D.C., USA
hgnami@fulbrightmail.org

ABSTRACT

Detailed palaeomagnetic studies were performed in several archaeological and geological sections dated with diverse relative and absolute methods. Data from 360 cores obtained in eight sites across eastern Argentina are reported. Characteristic remanence magnetization directions were determined by progressive alternating field demagnetization. Remanence directions showed anomalous geomagnetic field behavior far from the present magnetic field bearing oblique normal, oblique reverse and reverse polarities for the latest Pleistocene and Holocene, as well as evidence of possible field excursions recorded in several stratigraphic sections spanning ~11-0.5 kya. Computed virtual geomagnetic poles from those directions tend to be concentrated over North America, Europe, Eastern Asia, Africa and Australia. The hypothesis of the anomalous geomagnetic field directions is probably related with ^{14}C fluctuations and solar activity.
Key words: Paleomagnetism, Geomagetic excursions, Archaeology, South America, Argentina.

NUEVOS REGISTROS PALEOMAGNÉTICOS HOLOCENOS DETALLADOS CON COMPORTAMIENTO ANÓMALO DEL CAMPO MAGNÉTICO TERRESTRE EN ARGENTINA

RESUMEN

Se realizaron estudios paleomagnéticos detallados en varias secciones sedimentarias arqueológicas y geológicas fechadas con diversos métodos de datación absoluta y relativa. Se reportan resultados obtenidos de 360 muestras recogidas en ocho sitios localizados en el este de Argentina. La magnetización remanente característica fue determinada por desmagnetización progresiva utilizando campos alternos. Las direcciones remanentes mostraron conductas anómalas del campo geomagnético lejanas al campo actual mostrando polaridades oblicuas normales, oblicuas reversas y reversas con evidencia de posibles excursiones geomagnéticas registradas en varias secciones con un lapso temporal de ~11-0.5 kya. Los polos geomagnéticos virtuales computados a partir de las direcciones tienden a concentrarse sobre Norteamérica, Europa, Este de Asia, África y Australia. Se discute la hipótesis que la conducta anómala del campo magnético terrestre probablemente se relacione con las fluctuaciones de la producción de ^{14}C y la actividad solar.
Palabras claves: Paleomagnetismo, Excursiones geomagnéticas, Arqueología, Sudamérica, Argentina.

INTRODUCTION

Palaeomagnetic investigations on terminal latest Cenozoic deposits in Argentina have been a research subject since the early eighties (e. g. Creer et al., 1983; Valencio et al., 1985; Sylwan, 1989; Nami and Sinito, 1991; Sinito and Nuñez, 1997; Gogorza et al., 1998; 2000; etc.). Among these kinds of investigations, detailed research performed in

archaeological and paleontological sites in southern South America have yielded a number of records with anomalous geomagnetic field (GF) directions during the terminal Pleistocene and Holocene (Nami, 1995a; 1999a; Nami and Sinito, 1995; Sinito et al., 2001)**.** The anomalous GF behavior during the recent times seems to be an interesting palaeomagnetic issue, with important geomagnetic implications. Hence, to assess this topic a variety of sedimentary sections were sampled. Resulting from their study, this paper reports the results of a detailed palaeomagnetic research performed in archaeological and geological profiles corresponding to late Pleistocene and Holocene deposits. They belong to diverse continental sequences formed in tropical forest, fluvial, marine and cave's environments from eastern Argentina (Fig. 1).

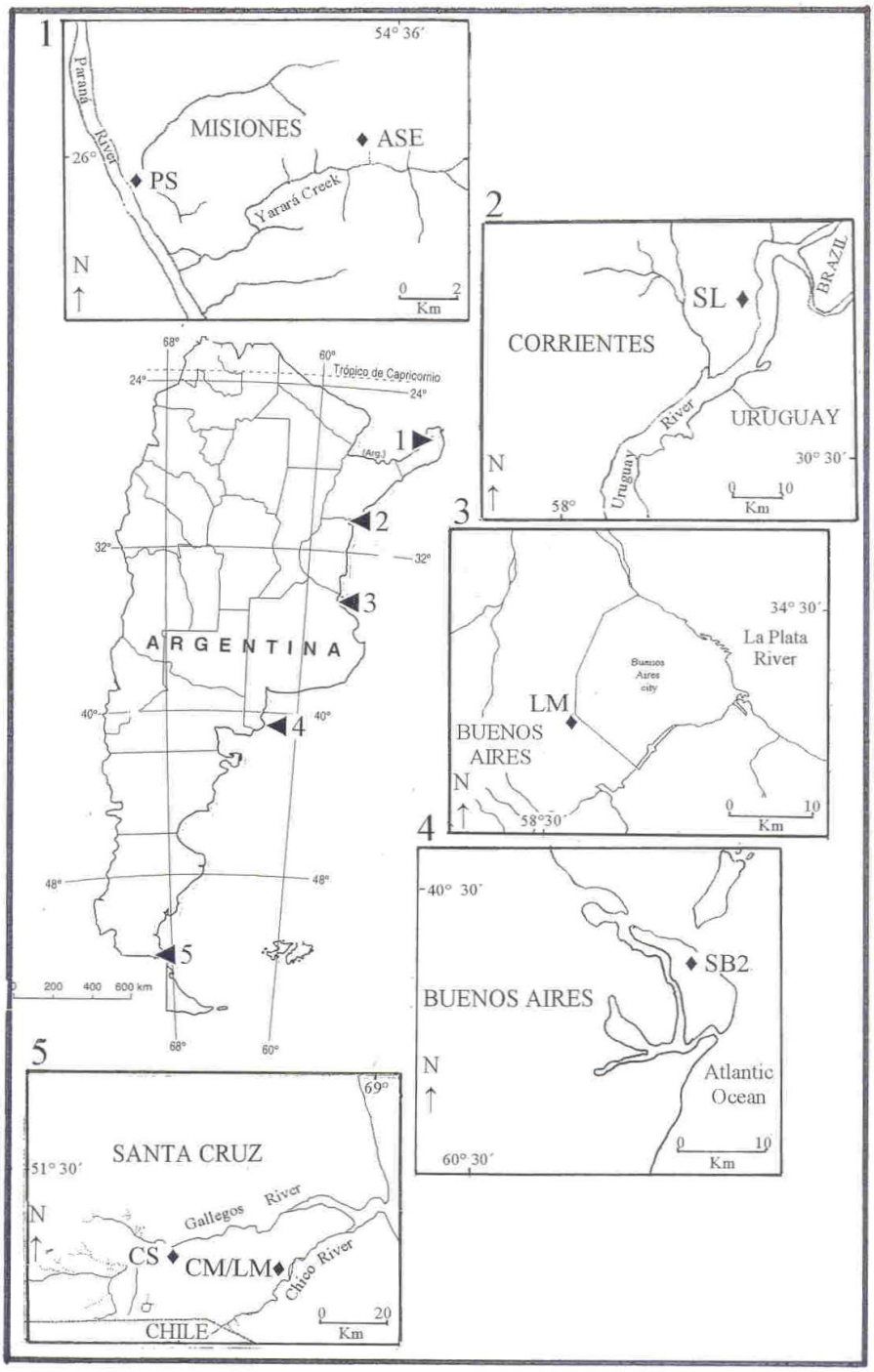

Figure1. Geographical location of the sites reported in this paper.
Figura 1. Localización geográfica de los sitios reportados en este artículo.

SAMPLING SITES AND AGE OF DEPOSITS

In order to check the palaeomagnetic results previously obtained, vertical paleomagnetic samplings were performed in sedimentary sections corresponding to the latest Pleistocene and to the Holocene. They are located in different regions from eastern Argentina (Fig. 1). The sampling sites are as follows:

Aserradero (ASE)

ASE (26° S, 54° 36.44' W) is an open air archaeological site located at Puerto Esperanza village, Misiones Province, NE Argentina. A ~0.80 m natural profile exposed during a street construction showed that archaeological artifacts in the whole deposit, including lithic waste and stone tools commonly called “cleaves curves” or bifaces with boomerang form. According to Brazilian archaeologists, these artifacts characterized the “Humaitá tradition” dated between ~7 and 1 ky bp (Schmitz, 1987). The sampling (n = 20) was obtained from a uniform red color sandy clay section (Fig. 2a).

Puerto Segundo (PS)

PS (25° 59.03' S, 54° 39.74' W) is situated near the Paraná River shoreline, at ~5 km east of ASE. A 1 m² by 1 m deep, trial pit in the sediments shows a stratigraphic level made up homogenous red sand. Archaeological remains were found in a discrete level with stemmed projectile points, lateral scrapers and very much lithic debitage, which might be comparable with those artifacts that characterize the “Umbú tradition” and ^{14}C dated between ~6-0.3 kybp (Schmitz, 1987; Rodriguez and Cerutti, 1999). Fifty samples were collected from a homogeneous red sand deposit that may correspond to Holocene. The archaeological level is located between samples 1 to 10 (Fig. 2b).

Santa Lucía (SL)

SL (30° 15.7' S, 57° 37.30' W) is located on the Uruguay river shoreline, 5 km south of Monte Caseros village, Corrientes province. Due to the quality and quantity of archaeological findings made in the earliest periods of the argentine archaeology, SL is a well-known place (Serrano, 1932; 1950). The archaeological findings occur in almost 500 m on the surface along the Uruguay River shoreline. Test pits revealed that archaeological remains occur from the surface down to approximately 1.10 m deep.

The sampled profile is 2.90 m thick and 1.50 m wide. Five natural strata can be seen, i.e. I, II, III, IV and V (Fig. 2c). Level I is mostly made up of sand and pebbles, whereas II, III and V are black, dark brown and brown clays respectively. Sediments yield abundant fine-grained quartz with subordinate calcium carbonate with cubic structure (Smorczewski, 1994). Level IV, on the other hand, appears to be volcanic ash layer that supposed to be regionally dated as ~10-11 ky bp (Miller, 1987). Therefore, the sampled section belongs to Late Pleistocene and Holocene. The sampling (n = 84) was carried out in the Northern profile; samples SL 1 to 31 were taken from level II, SL 32 to 58 from level III, SL 59 to 66 from level IV and 67 to 84 from level V. Archaeological artifacts from SL are similar to those founded at PS, suggesting a similar age of the deposit. It is impotant to point out that nearby SL, the Barranca Pelada site (Fig. 1), show a similar stratigraphy (Nami, 1999a; 2011). In SL, an AMS radiocarbon date from a very small sample of organic sediment obtained 90 cm deep in level II was dated as 3160 ± 35 yr B.P. (CURL-5506). Such age date was obtained from the humic acid fraction of the sediment, which tends to provide more reliable ages for this kind of materials (Pessenda, et al. 2001). However, this should be considered as a minimum age because the apparent mean residence time of organic components is a significant factor in soil dating (Scharpenseel, 1971; Stein, 1992).

Lomas del Mirador (LM)

LM (34° 39.29’ S, 58° 32.17 W) site is located in the outskirts of Buenos Aires City (Fig. 1). Despite that in this location there is presently no evidence of fluvial activity, sediments would correspond to the floodplain of the Maldonado creek basin, a significant water course existing in the historic Buenos Aires city fluvial system (Castellanos, 1975). The deposit show five stratigraphic levels named “I” to “V” (Fig. 2d); “I” corresponds to an artificial landfill, “II” to very dark brown highly compacted silt sediments, “III” to a dark brown silty clay level, “IV” to pale brown silty sand sediments, and “V” to a light yellowish brown silty clay deposit with calcareous inclusions. Levels II to V belong to a soil formation horizon (Nami, 2006). Two vertical paleomagnetic samplings sites identified as LM1 (n = 79) and LM2 (n = 70) were carried out in the northern and southern profiles respectively. LM1 sampling was performed from level II (samples LM1 1 to 9 and LM2 1 to 12), level III (LM1 10 to 52 and LM2 13 to 47), level IV (LM1 53 to 72 and LM2 48 to 70) and level V (LM1 72 to 79).

The age of the deposit was determined using different dating methods. Two ^{14}C dates on shell samples using mass accelerator spectrometry (AMS) were made. A small piece of unidentified mollusk from level II contains more ^{14}C than the 1950 atmosphere and therefore, can be considered as "modern". That is $\leq$1950 AD, which agrees with the age of the artificial landfill. The second age, obtained from one specimen of redeposited micro faunal mollusk (*Mactra isabelleana*) belonging to the lower part of level III. The date for this sample was 4900 ± 110 yr bp (OS-24330), in coincidence with those radiocarbon dates obtained from *Mactra isabelleana* collected from other sites in the region (Tonni et al., 1999). Additionally, the mean residence time (MRT) of the soil was determined employing the oxidizable carbon ratio (OCR) method (Frink, 1992; 1994; 1995). The MRT is the mixing of the young organic carbon with organic carbon from earlier stages of pedogenesis (Scharpenseel, 1971; Stein, 1992). Twelve OCR dates were obtained from levels II to V ranging between 110 and 7756 years bp (0.11-7.78 kybp) are as follows: 110 Act # 2943 (Act # 2943), 789 (Act # 2944), 1374 (Act # 2945), 3110 (Act # 2946), 4546 (Act # 2947), 5525 (Act # 3230), 6065 (Act # 3360), 6139 (Act # 3228), 6609 (Act # 3362), 6836 (Act # 3234), 7165 (Act # 3363), and 7556 (Act # 3229). Taking into account the radiometric date, these ages must be considered as relative minimum. Although there are notably differences between ^{14}C and OCR dates according to depth, the MRT suggests that the site was open to organic material deposition during the last ~8 ky; trough much of the Holocene, suggesting the Late Pleistocene/Holocene age. In fact, its boundary with the Pleistocene was conventionally established at 10 kyr bp (Dawson, 1992). In summary, based on geological and chronological studies it is possible to suggest that the magnetic signal reported in this paper belongs to the Holocene. A detailed study of this deposit is given in other papers (Nami, 2006; Vázquez and Nami, 2006).

San Blas 2 (SB2)

SB2 (40° 33.39' S, 62° 14.35 W) is placed at San Blas village, Jabalí island, SE Buenos Aires province, northern cost of Patagonia (Fig. 1). The sampling (n = 36) was carried out in a section exposed on the entrance road to the village. It showed five stratigraphic levels (Fig. 2e); three of them are fine sediments (numbered I to III) while the other ones, are two gravel layers, named as I and II. Gravel I is located under the vegetation and gravel II of about 16 cm thick, is between 0.94-1.10 m deep. Layer I is made up of sandy brown pale sediments, II of a more compacted sandy gray level and III of a reddish sand, located below gravel II.

The samples were taken as follows: In level I (samples SB2 1 to 18), level II (SB2 19 to 26) and the upper portion of level III (SB2 27 to 36). A sample of re-deposited shell coming from gravel II yielded a 14C date of 9720 ± 220 (LP-1006); other ^{14}C dates on gravel deposits from Jabalí island yielded ages of ~5.3 ky bp (Trebino, 1987). The gravel layer was probably formed at the time of the Holocene marine ingression that in the eastern coast of South America exhibited the maximum level between 6 and 5 ky bp (Isla, 1989; Schnack, 1990; Pirazzolli, 1996).

Cueva Montecarlo (CM)

CM (51° 54.86' S, 69° 38.79' W) is a small cave formed in an ancient crater called Montecarlo hill at ~1 km west of Markatch Aike ranch, in the Gallegos-Chico River basin, Santa Cruz province (Fig. 1), southern Patagonia (Nami, 1995b; 1999b). Underlying the bedrock, the deposit of ~0.4 m is made up of three layers (Fig. 2f): layer 1 corresponds to dung, 2 to silt (Bayarski, pers. com. 1997), and 3 is mostly formed by ash charcoal product of human hearths. The latter layer contains a notably archaeological level with stone tools used by hunter-gatherers living in the area during the late Holocene (Bird, 1988; Nami, 1995b). A conventional ^{14}C date obtained at 50 cm from the ash layer yielded an age of 1040 ± 50 uncalibrated years BP (Beta-124706). Twelve paleomagnetic samples in two section named CM1 (n = 6) and CM2 (n = 6) were made in layers 2 (samples 1 to 3) and 3 (samples 4 to 6).

Laguna Montecarlo (LMo)

LMo (51° 55' S, 69° 39´ W) is a small temporary lagoon located at 2.5 km west from MC (Fig. 1). To check the records obtained from archaeological sites from the region, a 1 m^2 trial pit by 0.9 m deep was made in the central area of the lagoon. Only one stratum of a uniform grayish green clay was sampled (n = 23) up to 52 cm deep. The Holocene age of the deposit is interpreted on the basis that these sort of small lagoons have been regionally formed after the post glacial times (Grondona, 1975).

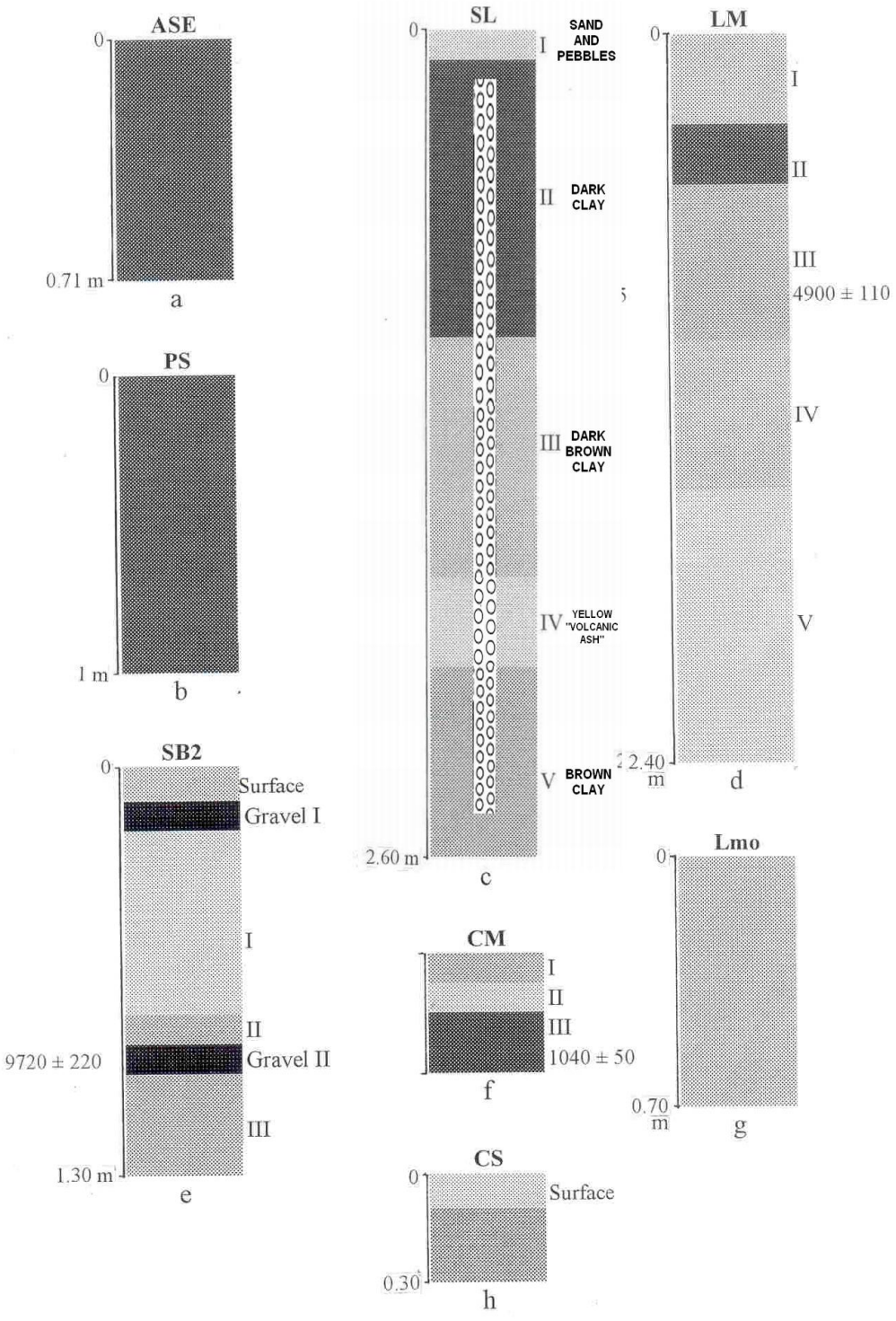

Figure 2. Schematic profiles showing the stratigraphic sections sampled related with ^{14}C dates. a) Aserradero, b) Puerto Segundo, c) Santa Lucía, d) Lomas del Mirador, e) San Blas 2, f) Cueva Montecarlo, g) Laguna Montecarlo, h) Cueva Saenz. Numbers to the right of the sections show numbers of layers, its sediments description and samples locations are given in the text.

Figura 2. Perfiles estratigráficos esquemáticos de las secciones muestreadas relacionadas con las fechas ^{14}C. a) Aserradero, b) Puerto Segundo, c) Santa Lucía, d) Lomas del Mirador, e) San Blas 2, f) Cueva Montecarlo, g) Laguna Montecarlo, h) Cueva Saenz. Los números en la derecha de las secciones indican los niveles, descripción sedimentario. La localización de las muestras están dadas en el texto.

Cueva Saenz (CS)

CS (51° 44.46' S, 70°09.92 W) located 60 km to the west of the Río Gallegos city (Fig. 1). This cave is located 400 m east of Las Buitreras cave, which was previously sampled (Nami, 1999a). Two palaeomagnetic samplings were performed in two parts of the site with different sedimentary deposits; one in the front part and the other in the inner portion. Here, only the preliminary results are reported, obtained in the cores (n = 5) taken from a ~30 cm sand level deposit located in the frontal part.

PALEOMAGNETIC STUDY

Sampling and laboratory procedures

As showed in figure 2c, samplings were done from the top to the base of the deposits in all sites. Samples were collected in 2.5 cm long and 2.5 cm diameter cylindrical bronze container in the case of SL. The other sites (ASE, PS, LM, SB2, CMo, LMo and CS) were sampled using 2.5 cm long and 2 cm diameter plastic containers. These were carefully pushed into the sediments with the precaution that they overlapped about 50%. Their orientation was measured using a Brunton compass; they were consolidated with sodium silicate once removed and finally, numerated from the top to the bottom. In some cases samples were not taken near the surface because the sediments were unconsolidated and could have been disturbed by recent events, such as animal and/or human trampling (CM). In other cases, despite that the section showed consolidation, the upper part seemed to be disturbed by roots (ASE, PS), the presence of pebbles and rocks (SL, CS) or because it was the result of an artificial landfill (LM).

All samples were subjected to progressive alternating fields (AF) demagnetization in steps of 3, 6, 9, 12, 15, 20, 25, 30, 40 and 60 mT in a 3-axis static degausser, attached to a 2G cryogenic magnetometer and subsequently measured with the magnetometer. Additional steps of 80 and 100, 120 and 140 mT were used in some samples. Previous experiments employing thermal cleaning in some sites (PS) or sediments from a similar deposit (Barranca Pelada site, which is ~ 10 km south of SL) showed that samples were highly unstable and hence, poorly reliable to isolate directions with this method (Nami and Sinito, 1995; Nami, 1999a; Sinito et al. 2001). By considering this, SL sediments were carefully removed from their containers and demagnetized with the AF method which was highly efficient in all the samples.

Characteristic remanent magnetization (ChRM) was calculated using principal components' analysis (Kirschvink, 1980).

RESULTS

Following the previous characterization of palaeomagnetic samples (Nami 1999a) according to the number of magnetic components and stability, remanence directions were qualified as: 1) "highly reliable" (HRe), with practically univectorial behavior with decay towards the origin (i.e. Fig. 3b, 4i, 8a), 2) "moderately reliable" (MRe), with "noisy" behavior during demagnetization and/or, well defined principal component but with erratic behavior during final steps (i.e. Fig. 7b, 9a), 3) "unreliable", with unstable behaviors (i.e. Fig. 11). All samples rated as 3) were rejected (n = 17). In general samples from each site display a common pattern with similar reliability. They are as follows:

ASE. Samples from this site showed a similar magnetic behavior. Most of them yielded orthogonal plots with one of two magnetic components (Fig. 3). In the majority, a ChRM could be defined trending towards the origin in the Zijderveld (1967) diagrams. Most of the secondary components corresponds to a soft viscous magnetic component that was easily removed between 3 and 12 mT (ASE5, ASE12, Fig. 3a, e). In most ASE cores less than 10% of the NRM was removed at 60 mT (Fig. 3). ASE8 and 20 (Fig. 3d, i) are examples of specimens with univectorial behavior with decay towards the origin. They have normal directions with low inclination values, whereas othes showed two components with the hard one decaying to the origin (ASE14, ASE16, ASE17, Fig. 3f-b). Several cores with reverse magnetization directions had a normal component that was removed at 20-25 mT (ASE7, ASE14, ASE 16, ASE17, Fig. 3c, f, g, h).

PS. By using AF demagnetization, most of the samples yielded HRe with linear decay towards the origin. Some specimens, however, showed a viscous component that was removed at 3-6 mT (PS 7, PS17, PS29, Fig. 4a, c). Vector projection diagrams (VPD) illustrated in Fig. 3 show samples with either single (PS 17, Fig. 4b) or more than one component with the anchored line of some of them decaying to the origin (PS37, PS42, PS44, Fig. 4d-f). Zijderveld diagrams show reverse (PS17, PS42, Fig. 4b, e) and normal polarities with either shallow (PS, Fig. 4d) or steep inclinations with north-easterly directions (PS7, Fig. 4a).

SL. In most cores less than 20% of the original intensity of magnetization remained at 80 mT (Fig. 5). The samples in figure 5 display similar behaviours with trajectories toward the origin in the Zijderveld diagrams (SL36, SL55, SL68, SL71, SL80, Fig. 5d, f-j). Other samples show trajectories that do not converge toward the origin (SL3, SL20, Fig. 3a) although the anchored line (McElhinny and McFadden, 2000). Most specimens had two magnetic components; some of them had an overprint of the present GF, which was removed around 3 to 6 mT (SL68 and SL80, Fig. 5h, j) while the other ones show two vectors, one of them was removed from 30-40 mT (SL3 and SL59, Fig.5a, g). Sample SL38 showed two components that could not be well isolated so that remagnetization circle analysis needed to be used (Fig. 5e, Fig. 10); such kind of sample were not used in this study. However, is significant to point out that its stereoplot illustrated in figure 10a shows that the vector changes from negative to positive inclinations (intermediate or reverse) moving in a great circle. The demagnetization curve depicted in figure 10b displays almost regular decay at 20% of the NRM up to 20 mT, however after a little remagnetization at almost 40% of the NRM remained at field of 140 mT. Many samples exhibit either steep (SL55 and SL80, Fig. 5f, j) or shallow negative inclinations (SL36, Fig. 5d). A few ones showed westerly (SL55, SL59, Fig. 5f-g) and northwesterly directions (SL68, SL71 and SL80, Fig. 5h-j). The detailed paleomagnetic research on SL site has been published in Nami (2011).

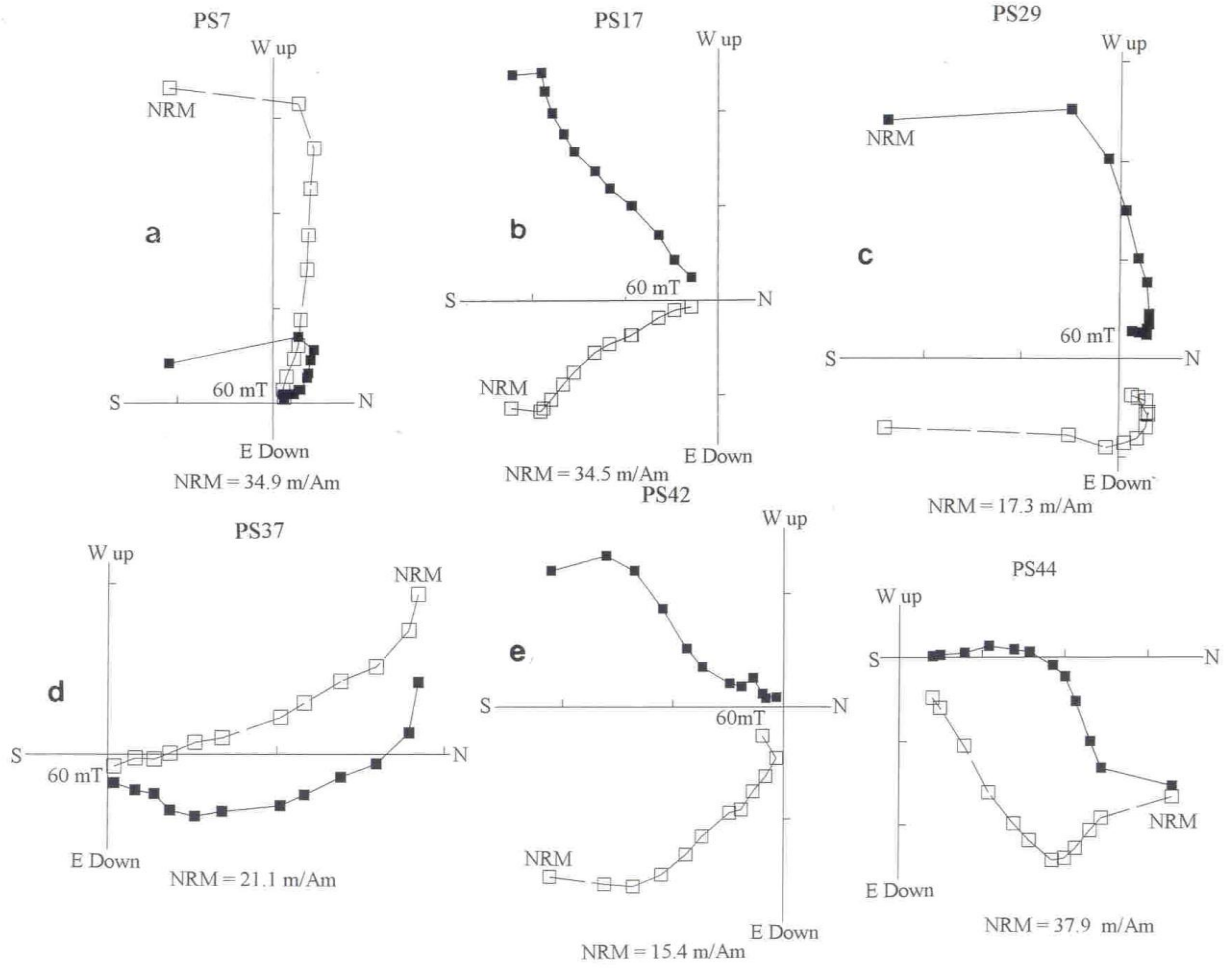

Figure 3. Typical Zijderveld diagrams from the PS section. Solid symbols correspond to the projection onto the horizontal plane, while open symbols are projection onto the vertical plane. The totality of the VPD illustrated in the figures are directional data with corrected field.

Figura 3. Diagramas de Zijderveld típicos de la sección de PS. Los símbolos en negro corresponde a la proyección horizontal mientras que los abiertos a la proyección en el plano vertical. La totalidad de los VPD ilustrados en las figuras son datos de direcciones con corrección de campo.

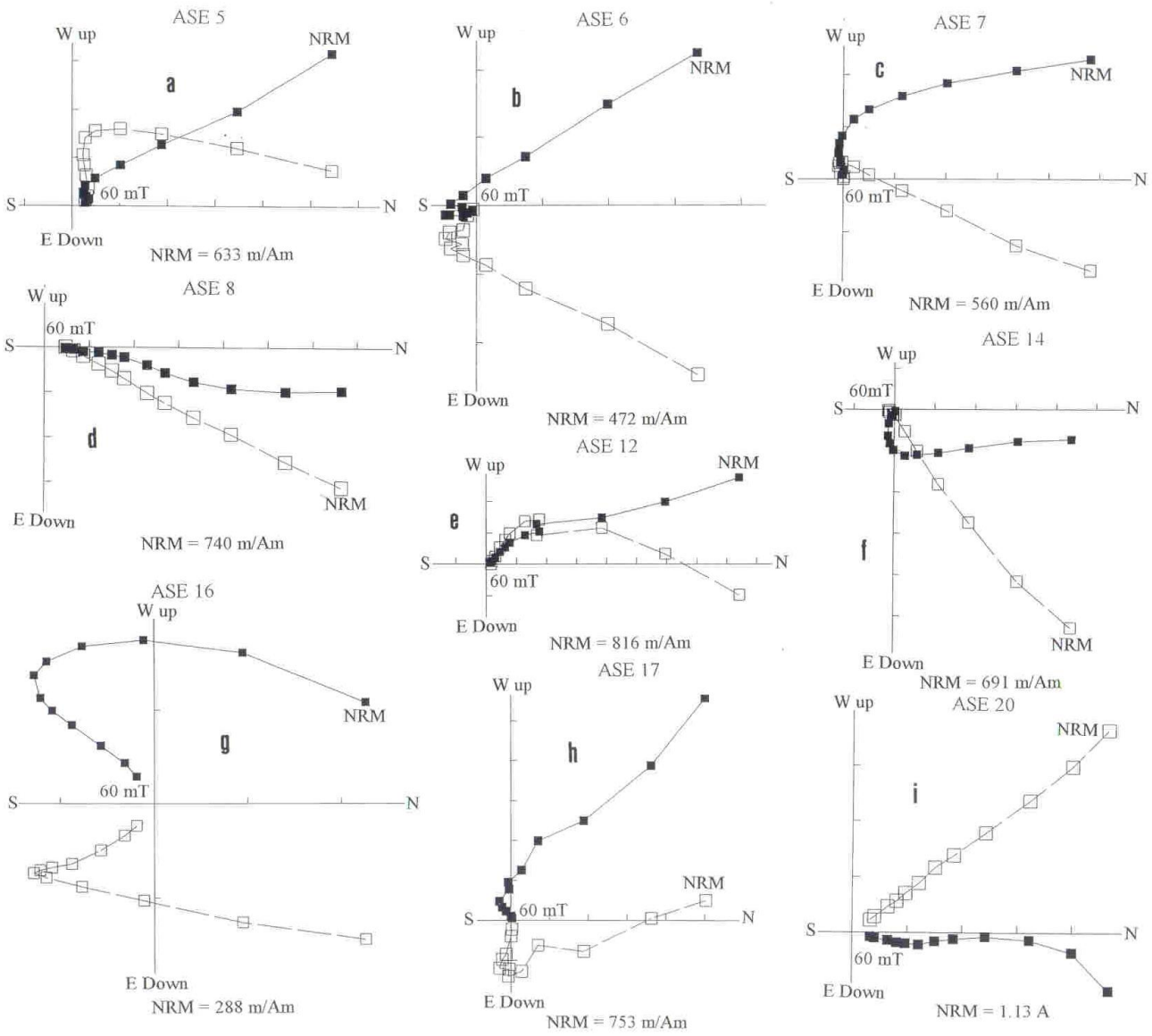

Figure 4. Vector components diagrams showing the behavior of typical samples from ASE profile.
Figure 4. Diagramas de components vectorial mostrando la conducta típica de las muestras del perfil ASE.

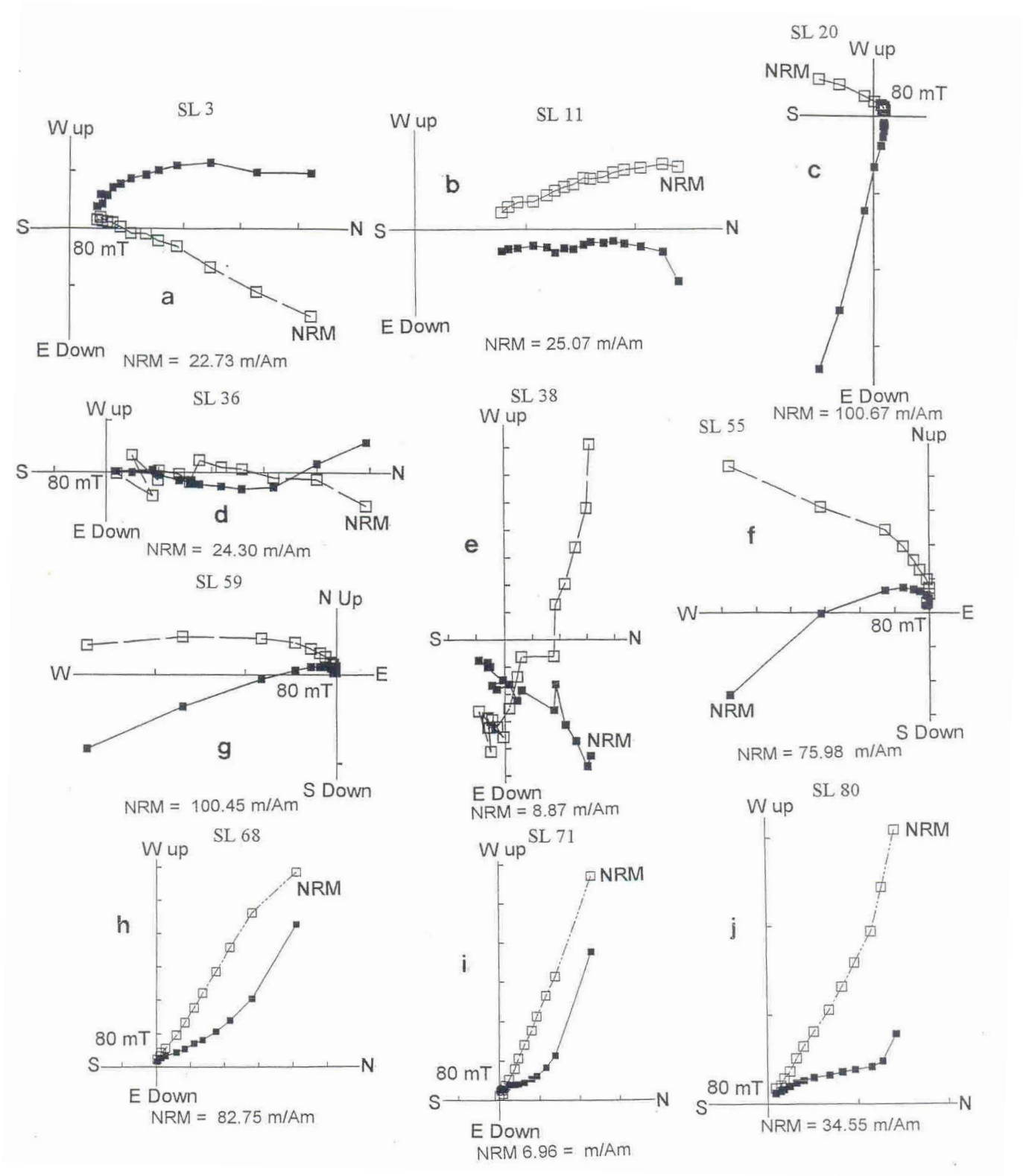

Figure 5. Examples of vector projection diagrams for SL site.
Figura 5. Ejemplos de los diagramas de proyección de vectores para el sitio SL.

LM. In most LM1 and LM2 cores less than 30% of the NRM remained at fields of 60 mT (Fig. 6a, b, e, g). Rock magnetic analysis from this section suggested that haematite is the principal carrier of the remanence with subordinate magnetite-titano-magnetite (Nami, 2006; Vázquez and Nami, 2006). Samples shown in figure 6 were highly reliable, displaying similar patterns of the trajectories going to the origin in the Zijderveld diagrams (LM1 10, LM1 19, LM1 54, LM2 6, LM2 24, Fig. 6b, d, f, j, k). Some samples had univectorial behavior (LM1 15, LM1 19 and LM2 1, Fig. 6c, d, h). The other ones had two magnetic components with the soft one coinciding with the present local dipolar field, which was removed between 3 to 6 mT (LM1 1 and LM2 5, Fig. 6a, i). The other samples showed two components, one of them was removed by 30-40 mT (LM1 30 and LM2 24, Fig. 6e, k). The ChRM show either steep (LM1 54, LM1 79 and LM2 24, Fig. 6f, g, k) or shallow negative inclinations (LM1 10 and LM2 5, Fig. 6b, i).

SB2. VDP diagrams depicted in Fig. 7 illustrates samples that showed a viscous remanence which was removed at 3-12 mT (e.g. SB2 3, SB2 16, Fig. 7a, c). The ChRM show cores with normal polarity directions with either steep (SB2 16, Fig. 7c) or shallow negative inclinations (SB2 8, Fig. 7b).

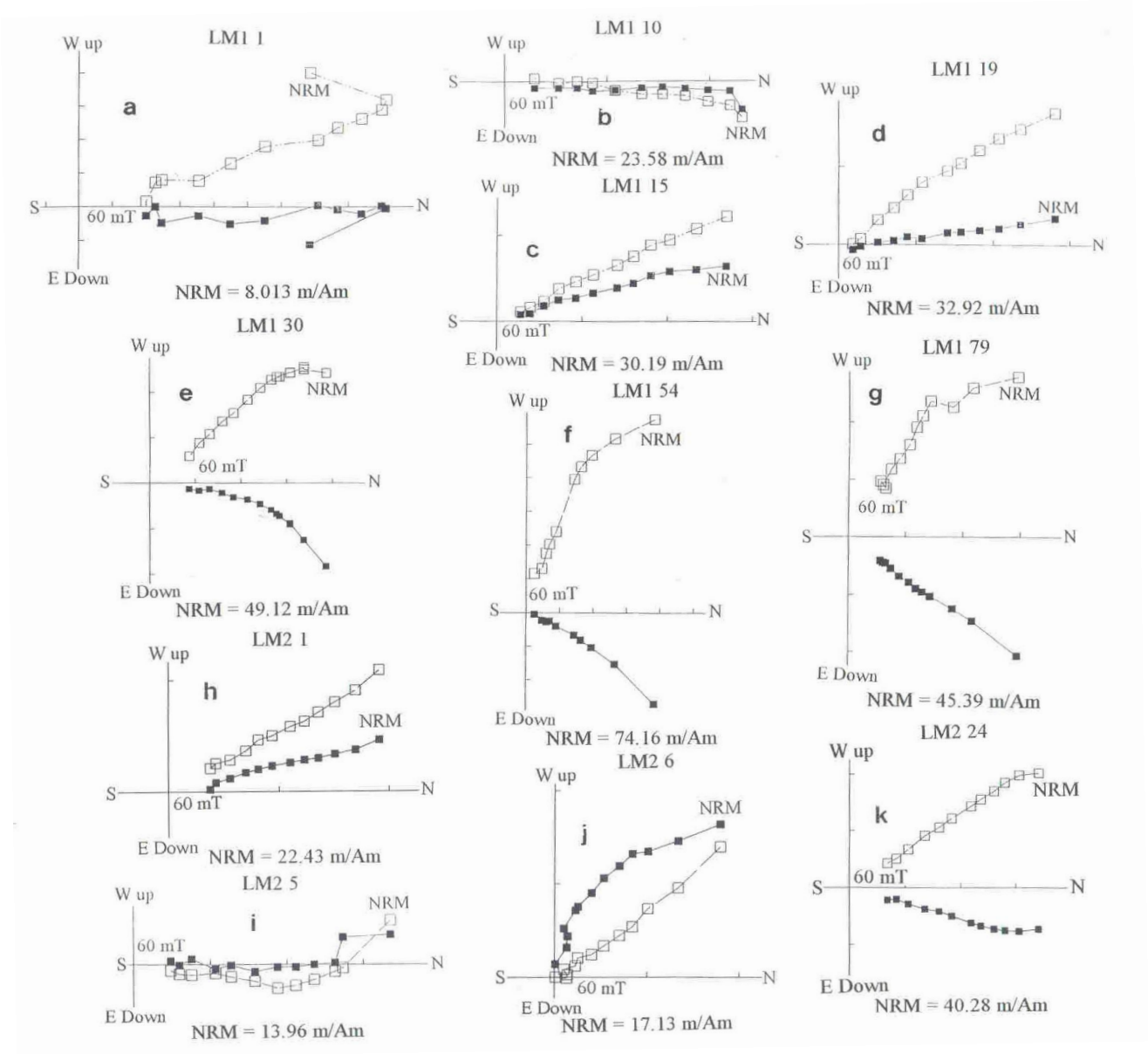

Figure 6. Typical Zijderveld diagrams from the LM1 and LM2 sections.
Figura 6. Diagramas de Zijderveld típicos de las secciones LM1 y LM2.

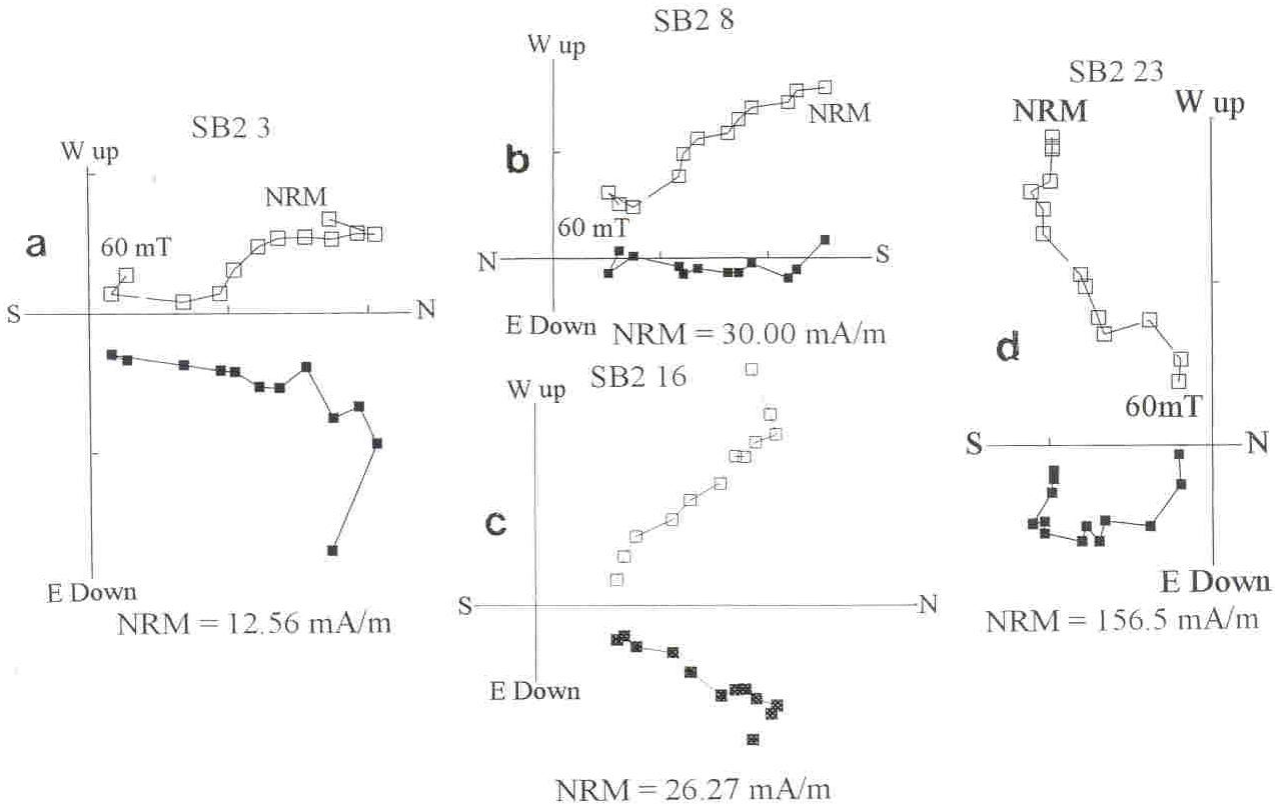

Figure 7. Zijderveld diagrams illustrating the SB2 magnetic behaviour.
Figura7. Diagramas de Zijderveld ilustrando la conducta magnética de SB2.

CM. Samples from this site showed similar magnetic behaviors. Most samples presented linear demagnetization plots with one of two magnetic components. The majority of the samples reveal a magnetic component trending towards the origin in the Zijderveld diagrams (CM1 2, CM1 4, CM2 1, Fig. 8a, b, d). Most secondary components were fully removed between 3 and 12 mT (CM1 3, CM2 4, Fig. 8b, f). Normal and oblique polarities (CM1 2, Fig. 8a), were found in several samples. In most CM cores less than 10% of the original intensity of magnetization was removed at 60-80 mT (CM1 2, CM2 2, Fig. 8a, e). CM1 2, CM1 4 CM2 1 (Fig. 8a, c, d) are examples of cores with univectorial behavior decaying towards the origin of coordinates with normal polarity directions (CM1 2, CM1 4, CM2 1, Fig. 8a, c, d), low inclination values (CM2 1, CM2 4, Fig. 8d, f). A few samples had two components with the second one decaying to the origin in the VPD diagrams (CM2 2, CM2 4, Fig. 8e, f).
LMo. The majority of the cores were highly reliable single components, displaying similar pattern going to the origin in the Zijderveld diagrams (LMo12, LMo16, LMo29, Fig. 9 b, d, e). Some samples had univectorial behavior with south- and north-westerly (LMo8, LMo21, Fig.9, b, e) and westerly directions (LMo1, LMo9, LMo10, Fig. 9a, c-d).
CS. The samples showed either single component remanence (CS5, Fig. 10b) and other ones had two magnetic components with anchored fitting line to the origin in the VPD diagrams; some cores showed a viscous remanence removed at 3 mT (CS1, Fig. 10a). They recorded univectorial reverse (CS16, Fig. 10b) and intermediate (CS5, Fig. 10a) directions.

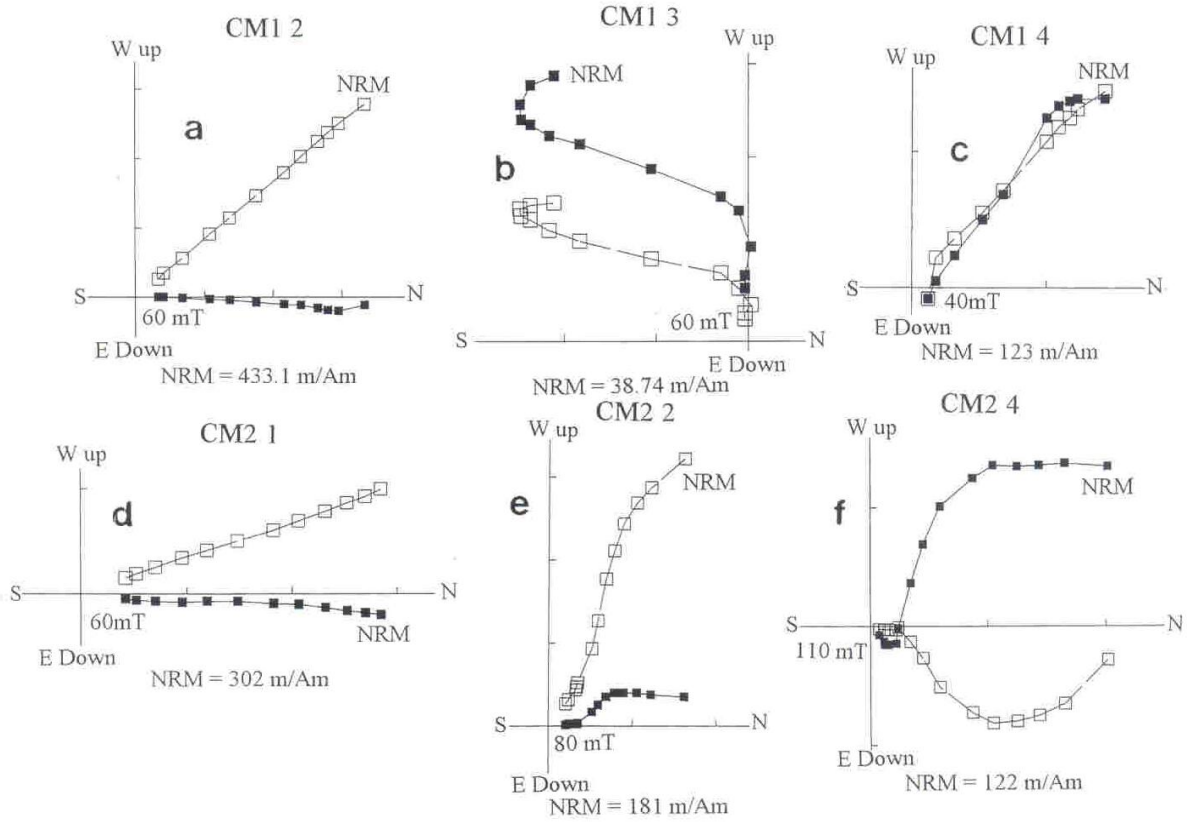

Figure 8. Examples of Zijderveld diagrams for CM section.
Figura 8. Ejemplos de diagramas de Zijderveld para la sección de CM.

All sections show normal and intermediate polarity directions far from the present local dipolar field, while reverse polarities were recorded at ASE, PS, and SB2. Figure 12 illustrates the stereographic projection of ChRM isolated from the sites under study. Figures 13 to 19 summarize the changes in the declinations and inclinations of the ChRM for the sections reported here. The more conspicuous long declination and inclination departures from SL and SB2 are depicted between dashed lines and indicated with arrows (Fig. 14 and 18).

ASE and PS also showed wide pulses in declinations and inclinations swings alternating positive to negative values in the whole sequence (Fig. 13 and 14). The overlapped stratigraphic presentation on both sections is presented in Figure 15. It can be seen that there is an interesting agreement between samples ASE1 and PS27 and ASE 20 and PS40. Relative chronologies for ASE and PS suggest that the observed GF anomalous behavior would have been taken place during the early and middle Holocene. This fact agree with the previously reported record located at ~1100 km west from both sites. Actually, Alero de las Circunferencias -a rock shelter sited in NW Argentina- also yielded logs with wide fluctuations alternating intermediate and reverse directions in the early Holocene at ~9-8 ky bp (Nami, 1999a).

SL deposit has a normal and oblique magnetic remanence with negative and positive low inclination values. The record of inclination presents a general decreasing trend from -80° at the lower part to 20° at the upper part (Fig. 16). The uppermost samples vary widely and there are transitional positions between the swings. An important oscillation in declination, that reaches values of approximately 40° to the east, is located between SL7 and SL46 samples. The samples recorded normal and intermediate polarity directions far from the present local dipolar field. A ~100° difference in inclination with low values mainly in the upper part of the section is observed. The declination record showed a significant westward shift with fluctuations occurred in the same portion. However, major swings in inclination are between samples SL25 to SL51, and SL48 and SL84 in declination. In Corrientes province and near SL, Barranca Pelada (BP) and San Juan (SJ) sites were previously analyzed. They also yielded normal and intermediate polarity positions during the Holocene (Nami, 1999a). These facts suggest that variations in the paleomagnetic records might

reflect the GF behavior, instead a reflection of noise in the magnetic recording process (Dunlop and Özdemir, 1997). Moreover, by overlapping the BP and SJ logs with SL, an inter-site correlation was done from the declination and inclination patterns. As depicted in Figure 17, they showed a remarkable agreement with the upper and middle part of SL. In fact, samples BP9 to BP40 agrees fairly well with SL5 to SL37 and SJ1 to SJ21 with SL18 to SL39 in that order.

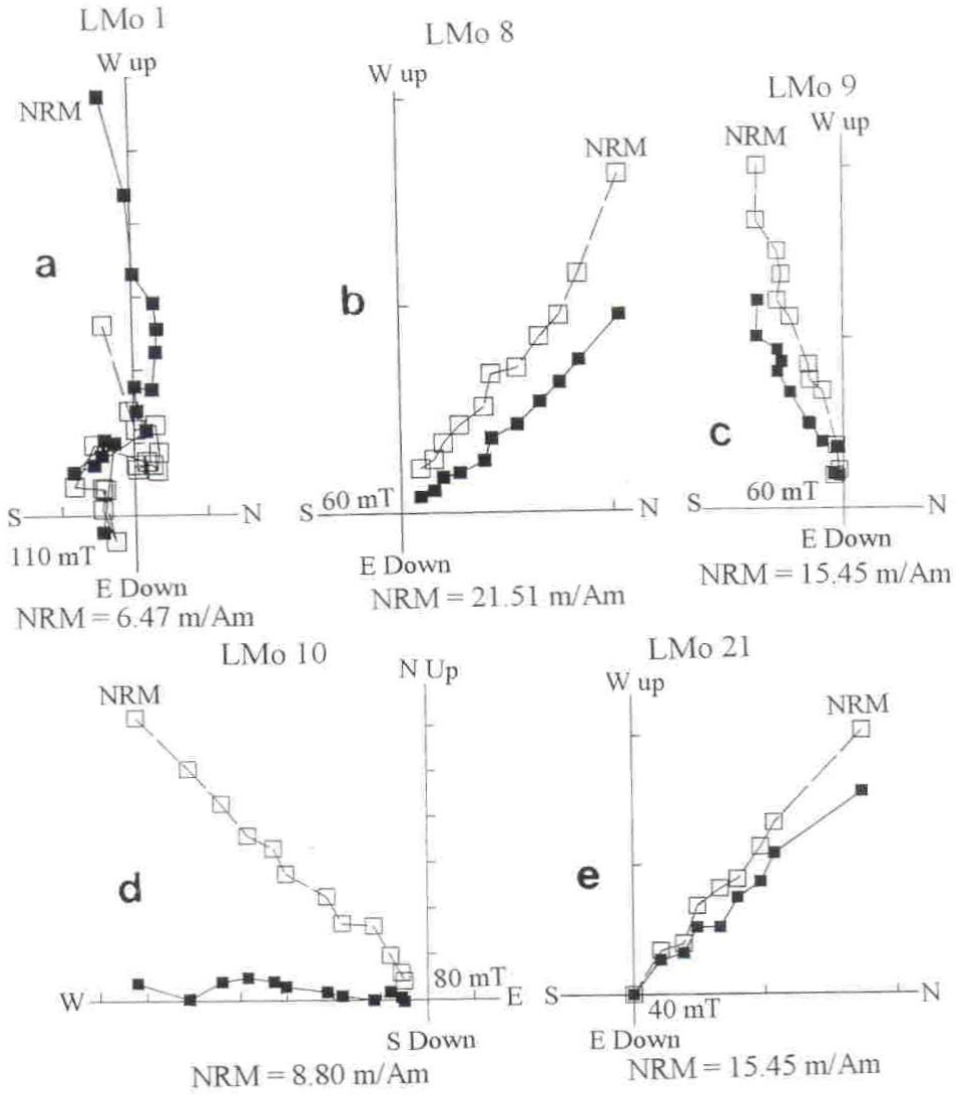

Figure 9. Vector components diagrams showing the behaviour of typical samples from LMo site.
Figura 9. Diagramas de components vectoriales mostrando la conducta de muestras típicas del sitio Lmo.

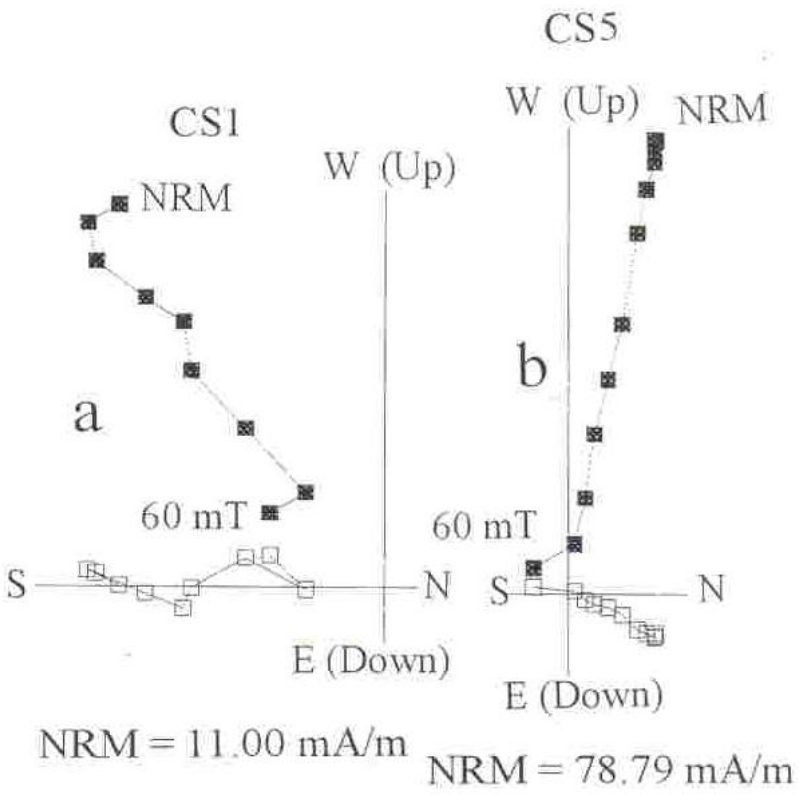

Figure 10. Examples of Zijderveld diagrams for CS site.
Figura 10. Ejemplos de los diagramas Zijderveld para el sitio CS.

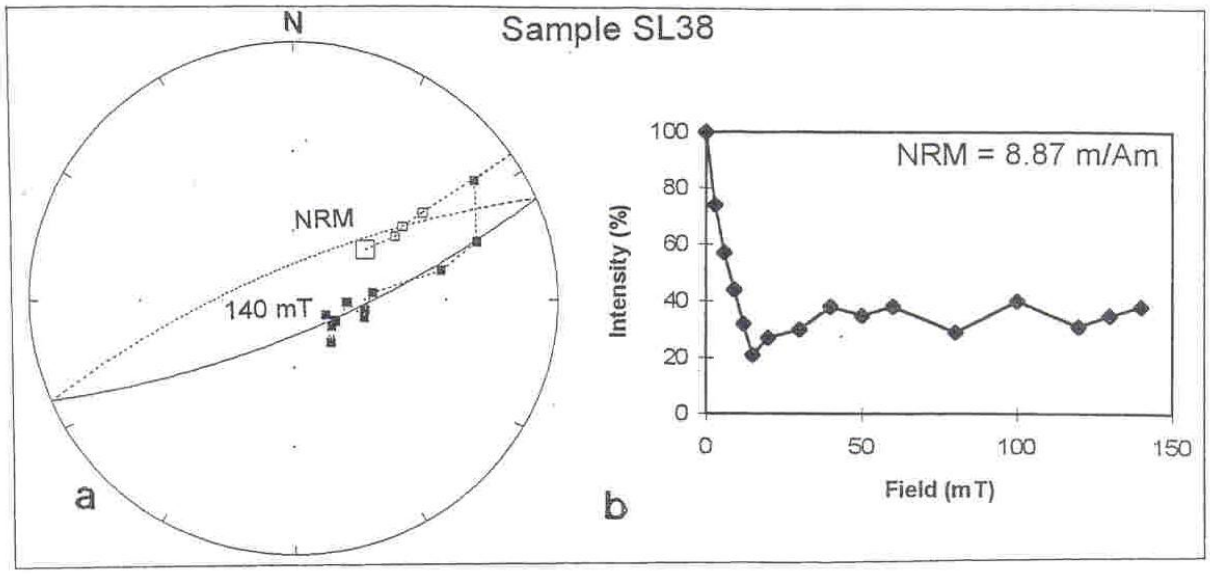

Figure 11. Example of unreliable multicomponent sample to isolate directions from SL (#38) moving in a maximum circle. A) Stereographic projection, B) Zijderveld diagram.
Figura 11. Ejemplo de muestra multicomponente no confiable (SL38) para aislar una dirección, la cual se mueve en un círculo máximo. A) Proyección estereográfica, B) Diagrama de Zijderveld.

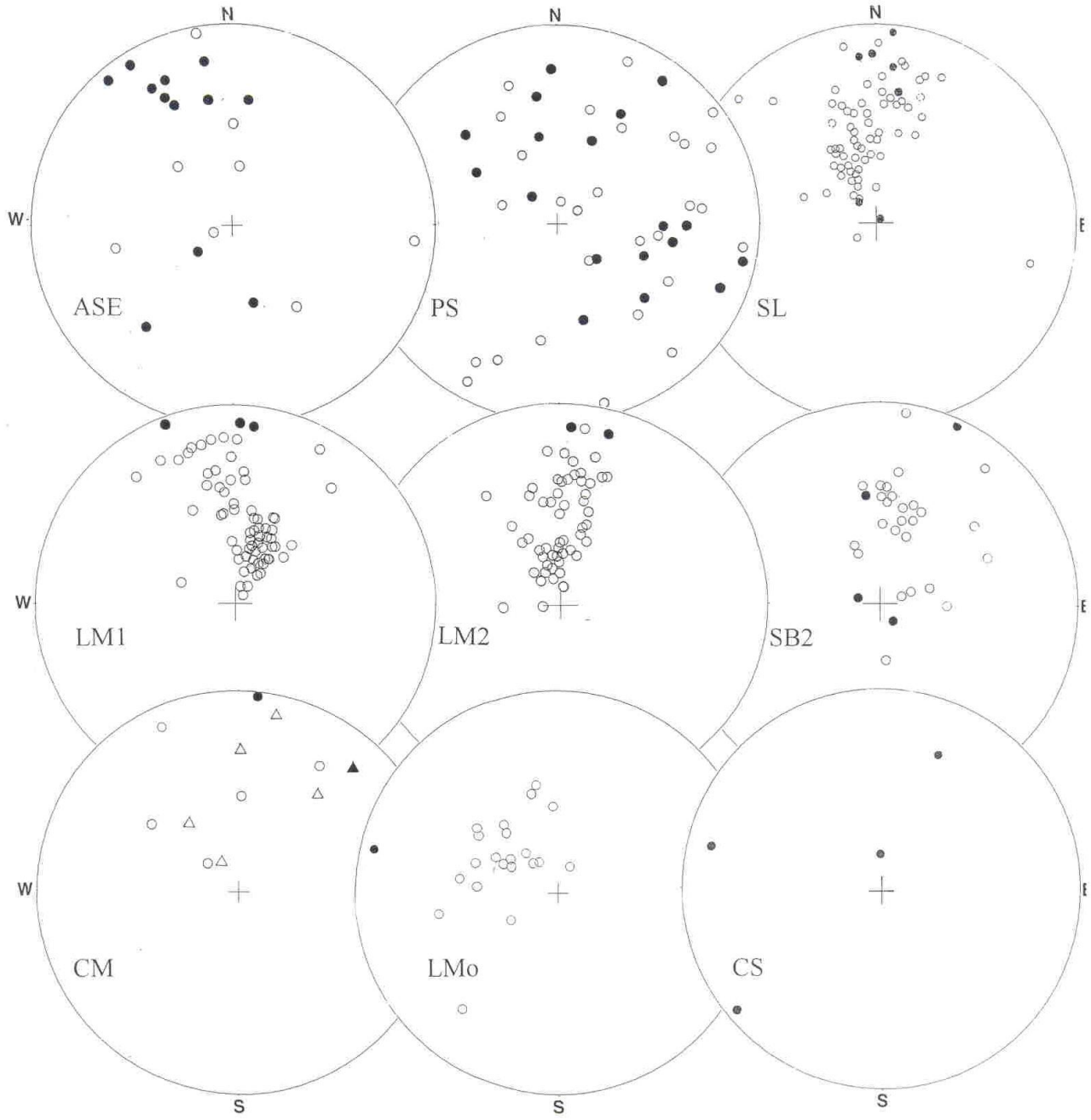

Figure 12. Directional data with field correction of characteristic remanent mangnetizations (ChRM) of each sample for the sections reported in this paper. Negative inclination (open circle) and positive inclination (solid circle).

Figura 12. Datos de direcciones con corrección de campo de la magnetización remanente característica (ChRM) de cada muestra de las secciones reportadas en este artículo. Inclinación negativa (círculo abierto) e inclinación positiva (círculo lleno).

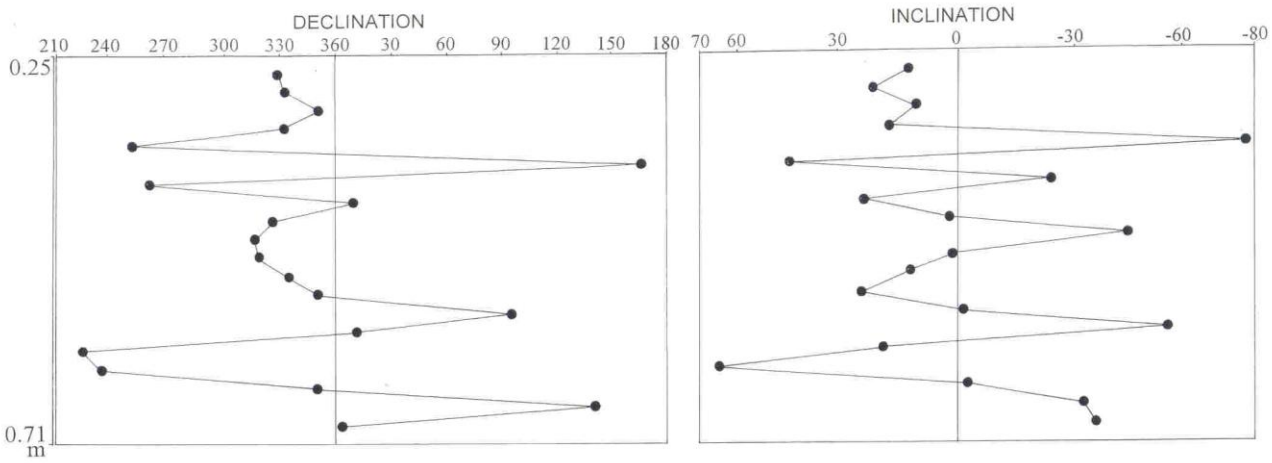

Figure 13. Declination and inclination logs from ASE site.
Figura 13. Registro de declinación e inclinación del sitio ASE.

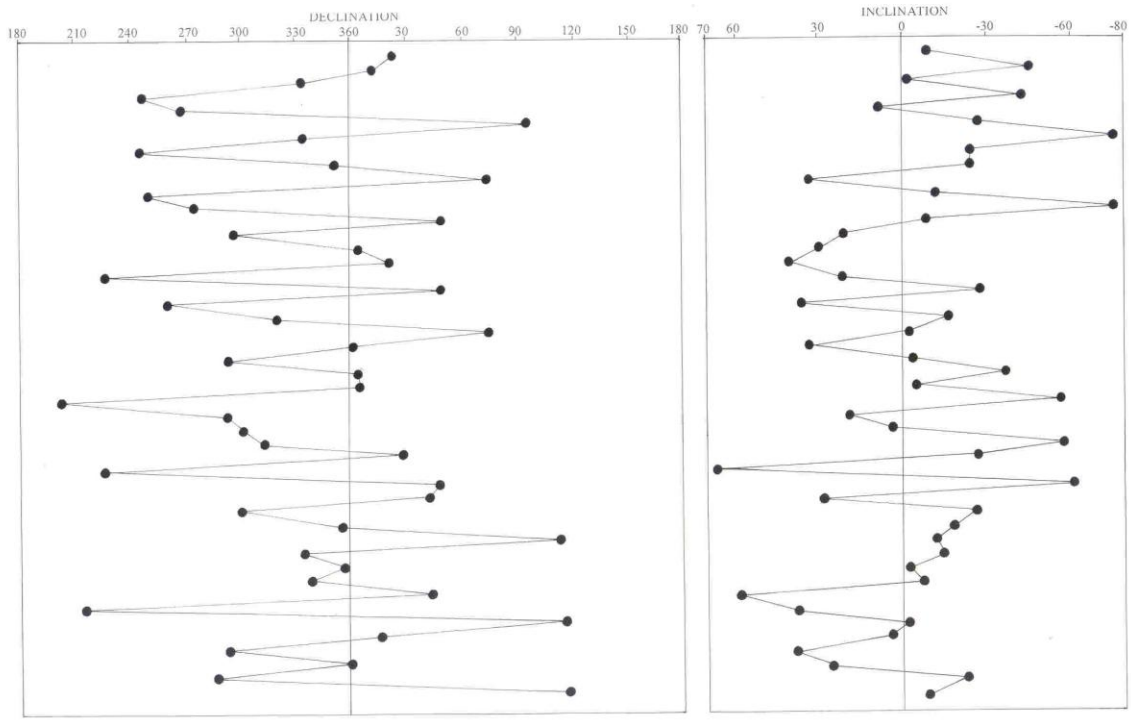

Figure 14. Magnetograms illustrating the Declination and Inclination logs for PS.
Figura 14. Magnetogramas ilustrando los registros de declinación e inclinación de PS.

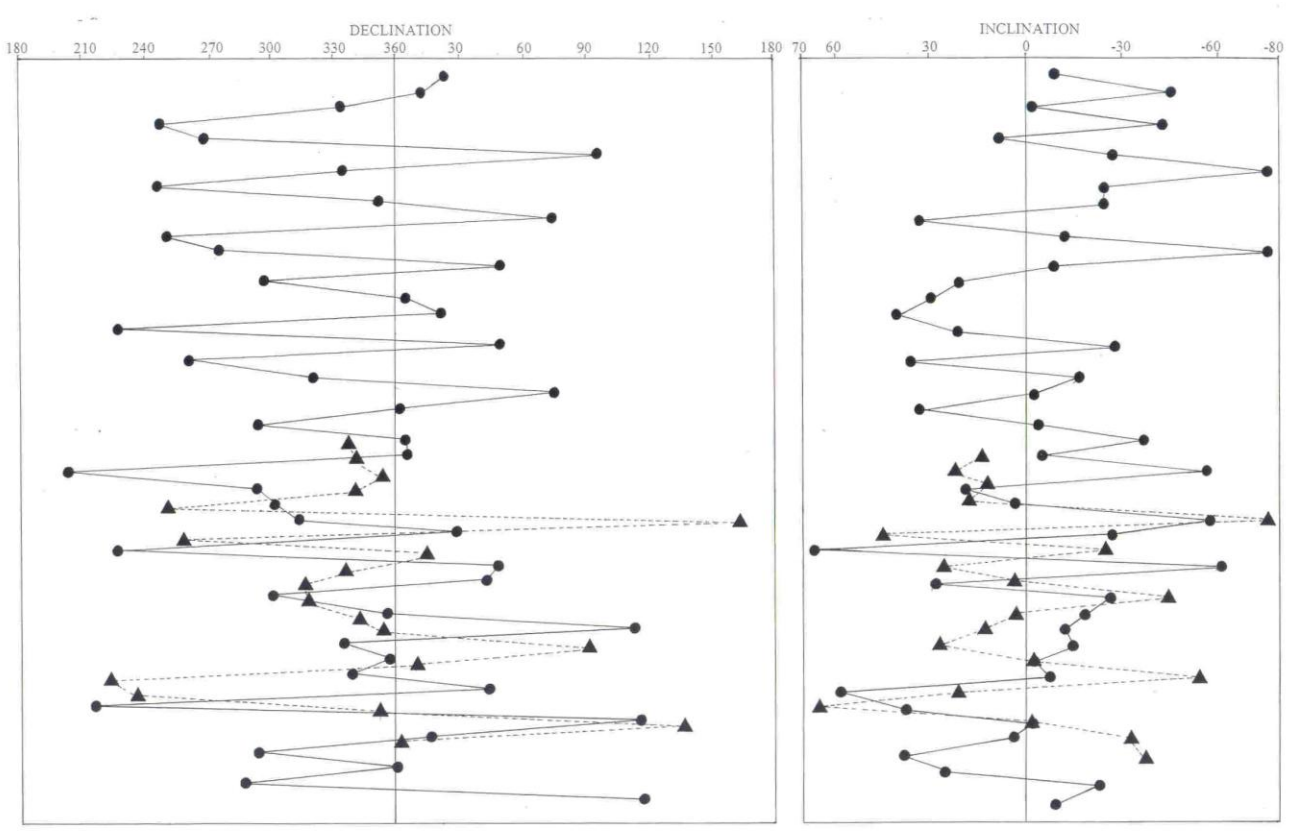

Figure 15. Overlapped stratigraphic presentation of Declination and Inclination logs from PS (solid circles) and ASE (solid triangles and dashed line)

Figura 15. Presentación traslapada de los registros de declinación e inclinación de PS (círculos llenos) y ASE (triángulos llenos y línea cortada).

LM sampling clearly shows a similar GF magnetic behavior with a conspicuous change in declination and inclination. An important swing in declination, which reaches values of approximately 100° to the West, is located between samples 1 to 32 in LM1 and 1 to 34 in LM2 (Fig. 18). Besides, the record of inclination record presents a general decreasing shift from ~80° at the lower portion to 10° at the upper part. The declination log has a general diminishing trend between 30° E at the bottom and 45° W at the top. The mean declination and inclination values from correlatives samples of both sampling sites were used to construct a smooth curve (Fig. 19). Samples 38, 52, 54, 58 and 69 were not considered in this analysis because their directions have more than 45° difference. Afterwards, this curve was compared with the mean directions from SL, BP and SJ (Fig. 20). There are remarkable similarities in the upper part of LM declination log and low inclination values during the late Holocene and probably in recent centuries (≤ 0.5 ky bp).

Figure 21 illustrates the stratigraphic presentation of the declination and inclination profiles from SB2, showing an important correlative shift toward higher negative values in inclination of ~40-50° between samples 1 and 16 in the upper portion of the section. The declination and inclination logs also shows wide pulses with reverse directions and transitional positions between samples 20 and 30. Similar situation occurred in other archaeological and paleontological sites previously reported, such as Mylodon Cave, Alero de las Circunferencias and Las Buitreras cave in Chile and Argentina (Nami, 1995; 1999a). SB2 records suggest a shift from normal to reverse positions during the early and middle Holocene (9-6ky bp).

In LMo a significant but gently westward shift in declination (over 90°) and less conspicuous shallowing of the inclination can be observed (Fig. 22a). Both samplings in CM recorded negative to positive changes in inclination with similar directions during the first millennium bp (Fig. 22b).

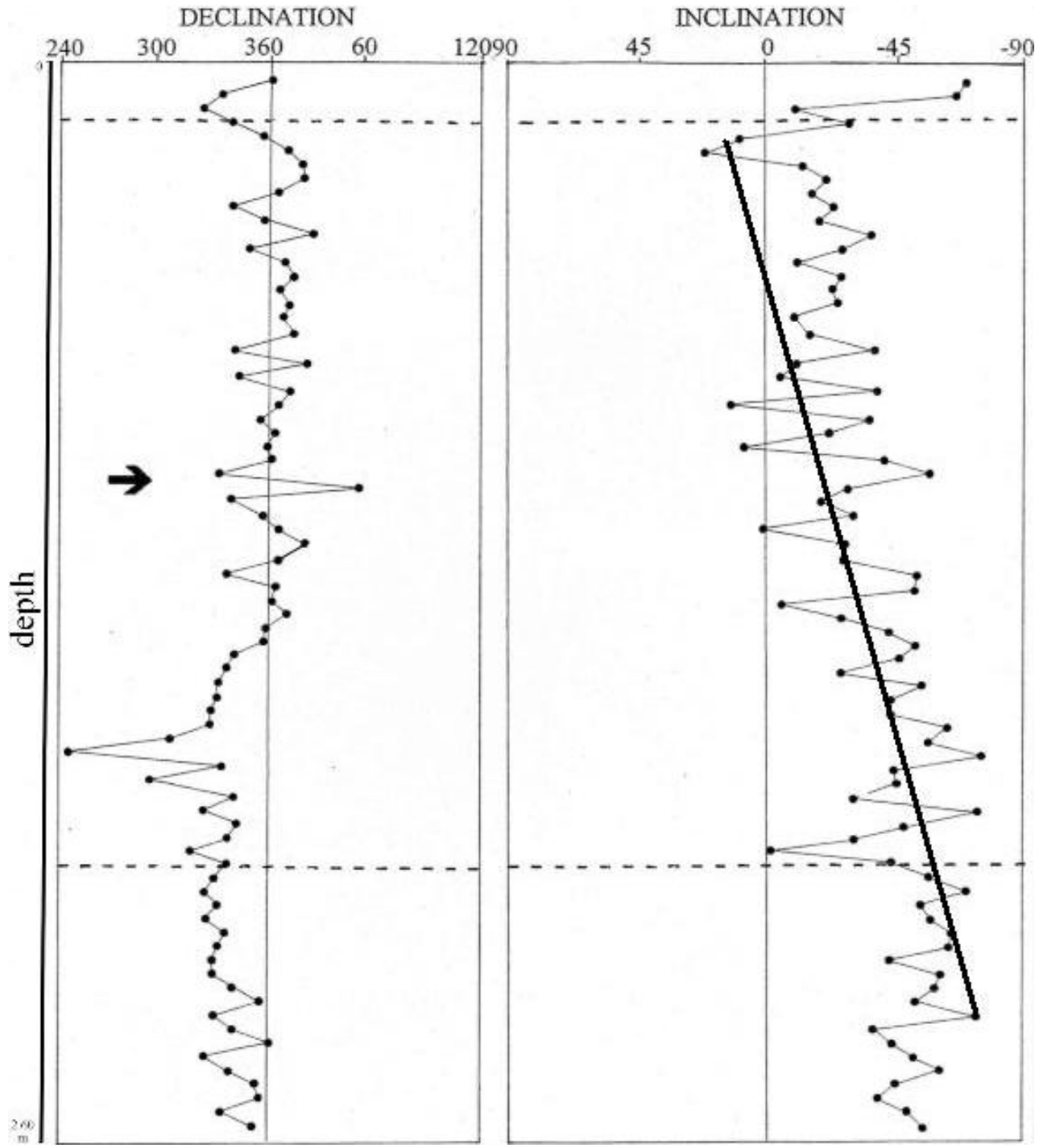

Figure 16. Stratigraphic presentation of the Declination and Inclination profiles from SL The more conspicuous long direction departures are depicted between dashed lines and pointed with an arrow. The line shows the decreasing trend from ~-80° at the lower part to ~20° at the upper part.

Figura 16. Presentación estratigráfica de los perfiles de declinación e inclinación de SL. Los apartamientos de direcciones más amplios se representan entre líneas de trazos y se señalan con una flecha. La línea muestra la tendencia a la disminución de ~ -80 ° en la parte inferior a ~ 20 ° en la parte superior.

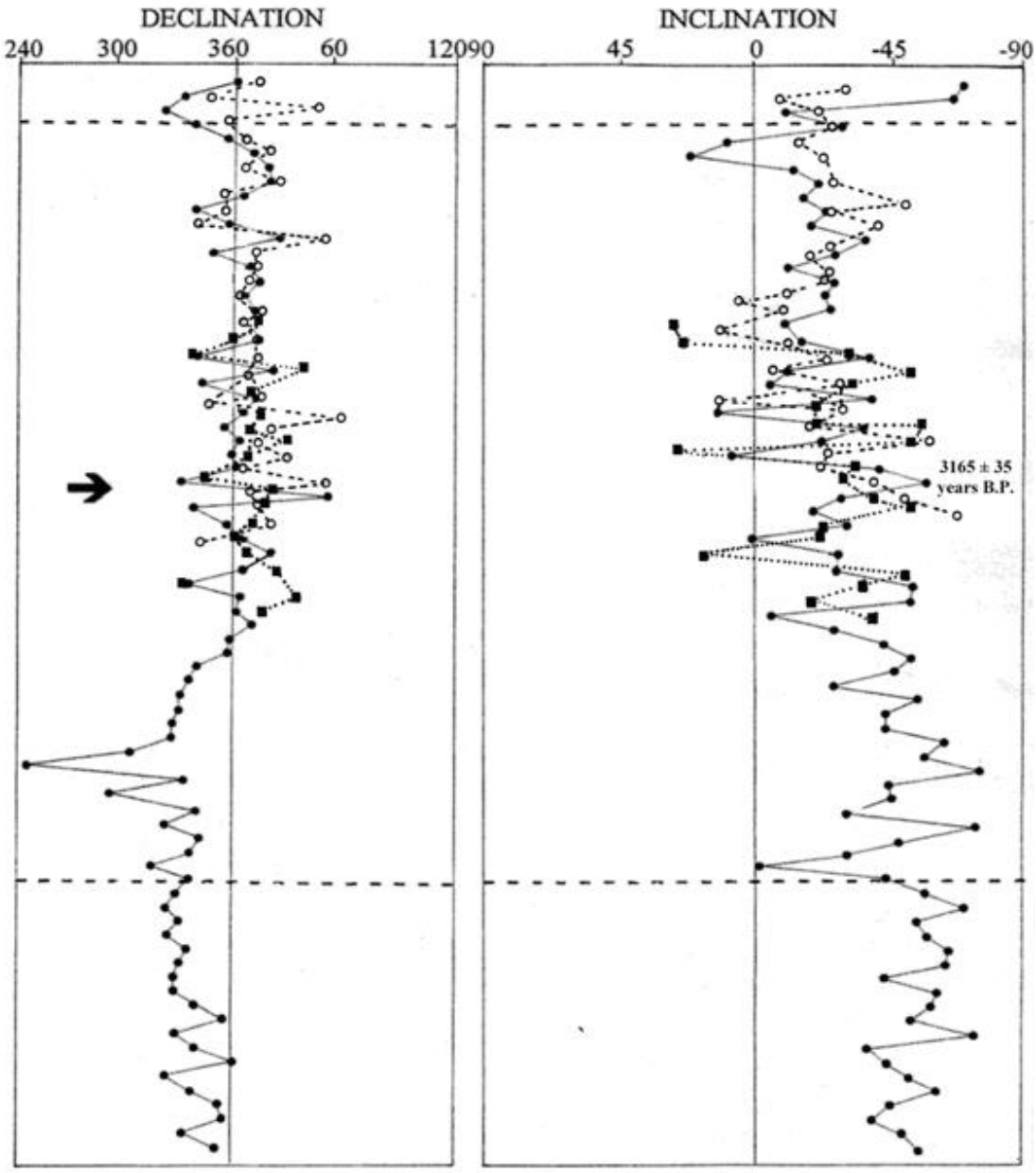

Figure 17. Overlapped stratigraphic presentation of SL, BP and SJ declination and inclination profiles related with the direct the absolute date by AMS obtained at BP; solid circles and continuous line: SL, open circles and dashed lines: BP, squares and pointed line: SJ. The more conspicuous long directions departures are depicted between dashed lines and pointed with an arrow.

Figura 17. Presentación traslapada de los registros de declinación e inclinación de SL, BP y SJ relacionados con la datación absoluta por AMS obtenida en BP; círculos llenos y línea continua: SL, círculos abiertos y línea cortada: BP, cuadrados y línea punteada: SJ. Las direcciones con apartamientos más conspicuos se muestran entre las líneas punteadas y se señalan con la flecha.

Despite the scarce number of cores reported here, CS shows similar directions than other sites from southern Patagonia in Argentina and Chile. In fact, previous results obtained at Mylodon, Cueva del Medio, Don Ariel and Las Buitreras caves yielded remanence directions corresponding to oblique normal, oblique reverse and reverse field polarity directions with similar VGPs. This situation strengthens the hypothesis of the real existence of anomalous GMF behavior during the terminal Pleistocene and Holocene in southern Patagonia (Nami, 1994; 1995a; 1999a; Nami and Sinito, 1995). On the other hand, the presence of intermediate and reverse VGPs in ASE, PS and SB2 also supports its regional extent in the southern part of South America. Others sites in Argentina that recorded low inclination values

during the late Holocene were SL, LM, BP, SJ, Piedra del Aguila 11, Campo Cerda (Nami and Sinito, 1991; 1993; Sinito et al., 1997; Nami 1999a).

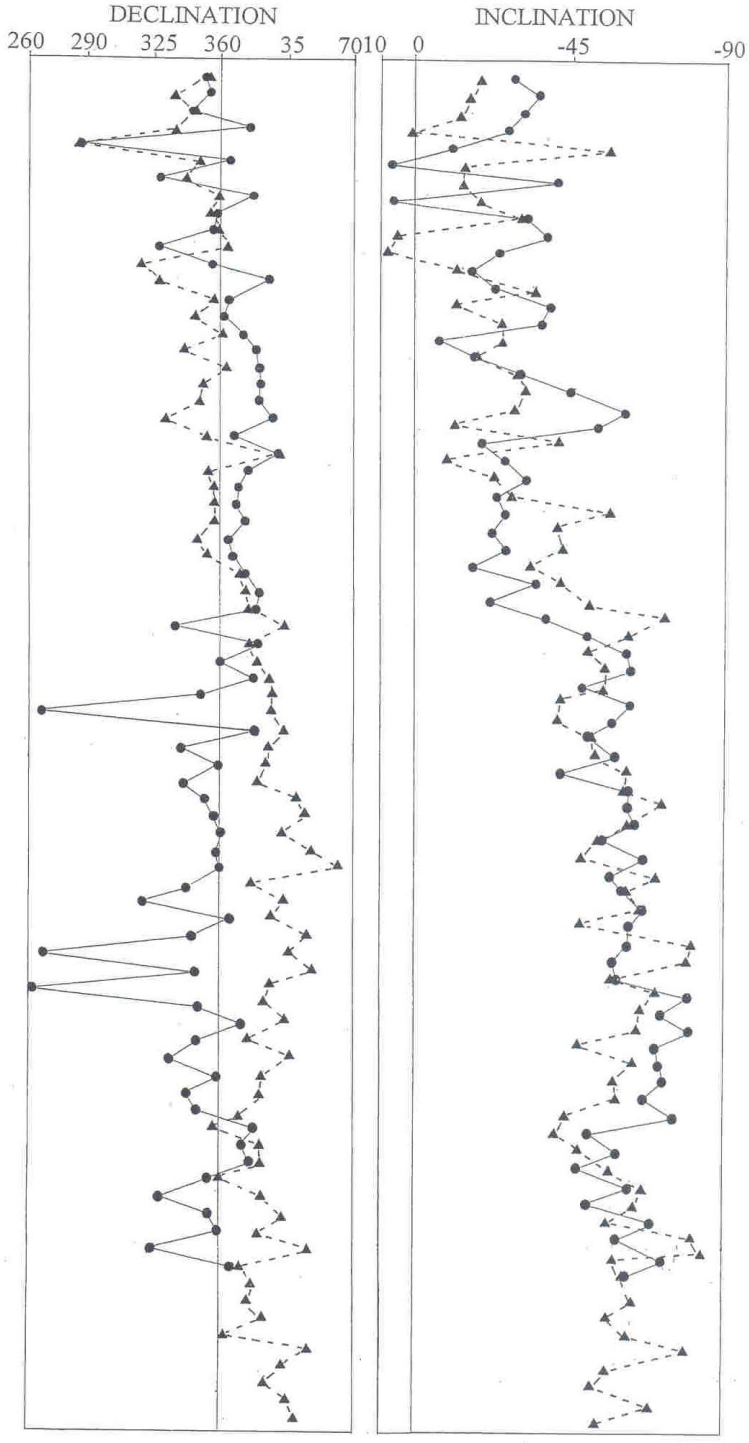

Figure 18. Stratigraphic presentation of the Declination and Inclination overlapped profiles from LM1 (solid circle) and LM2 (triangle and dashed line).

Figura 18. Presentación estratigráfica de los perfiles de declinación e inclinación sobrelapados de LM1 (círculo lleno) y LM2 (triángulo y línea cortada).

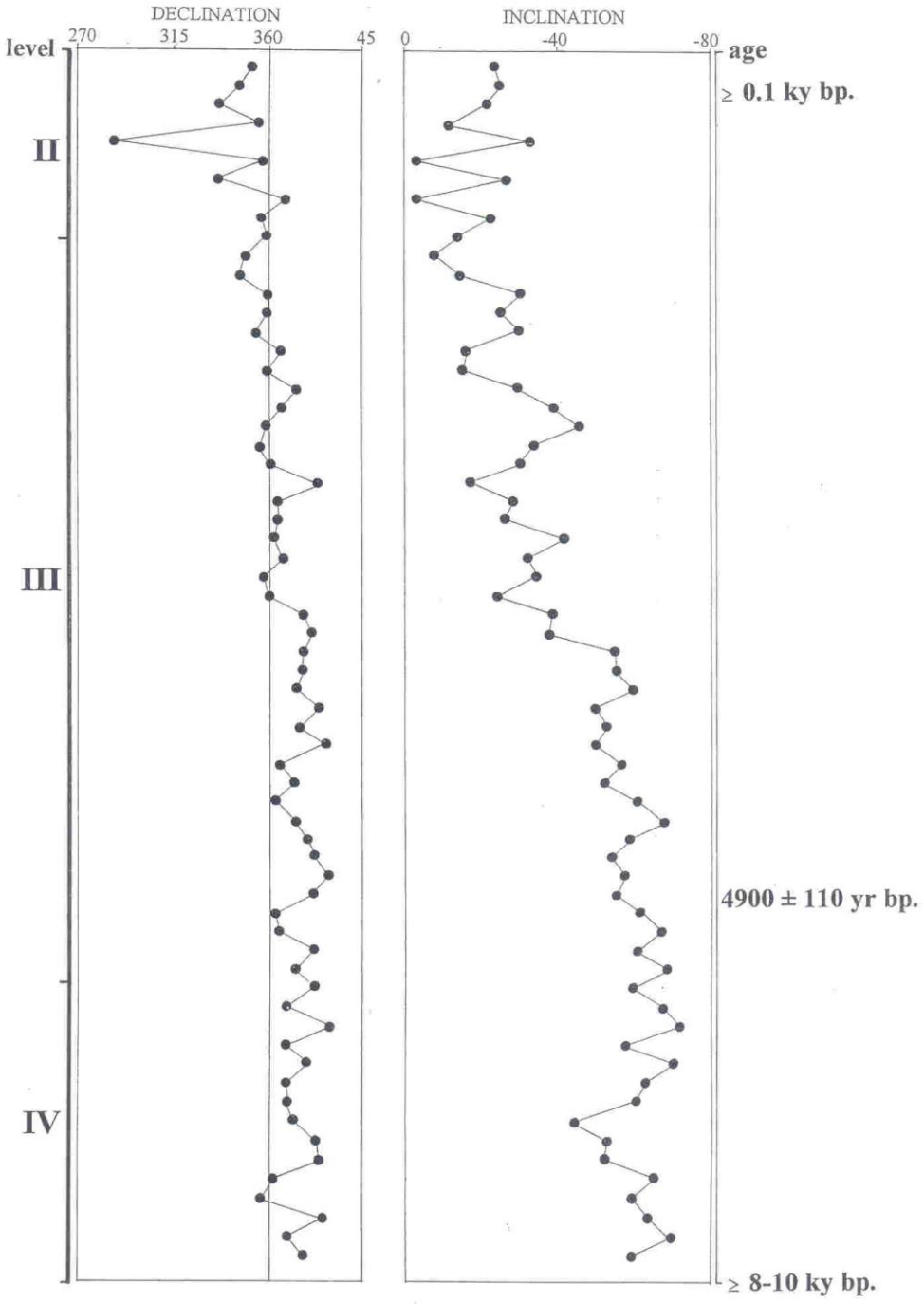

Figure 19. Stratigraphic presentation of mean Declination and Inclination profiles from LM1 and LM2 related with the stratigraphical section and relative and absolute ages. Samples with more than 45° difference were not averaged.

Figura 19. Presentación estratigráfica de los perfiles de declinación e inclinación media de LM1 y LM2 relacionados con la sección estratigráfica y la edad absoluta. Las muestras con más de 45° de diferencia no fueron promediadas.

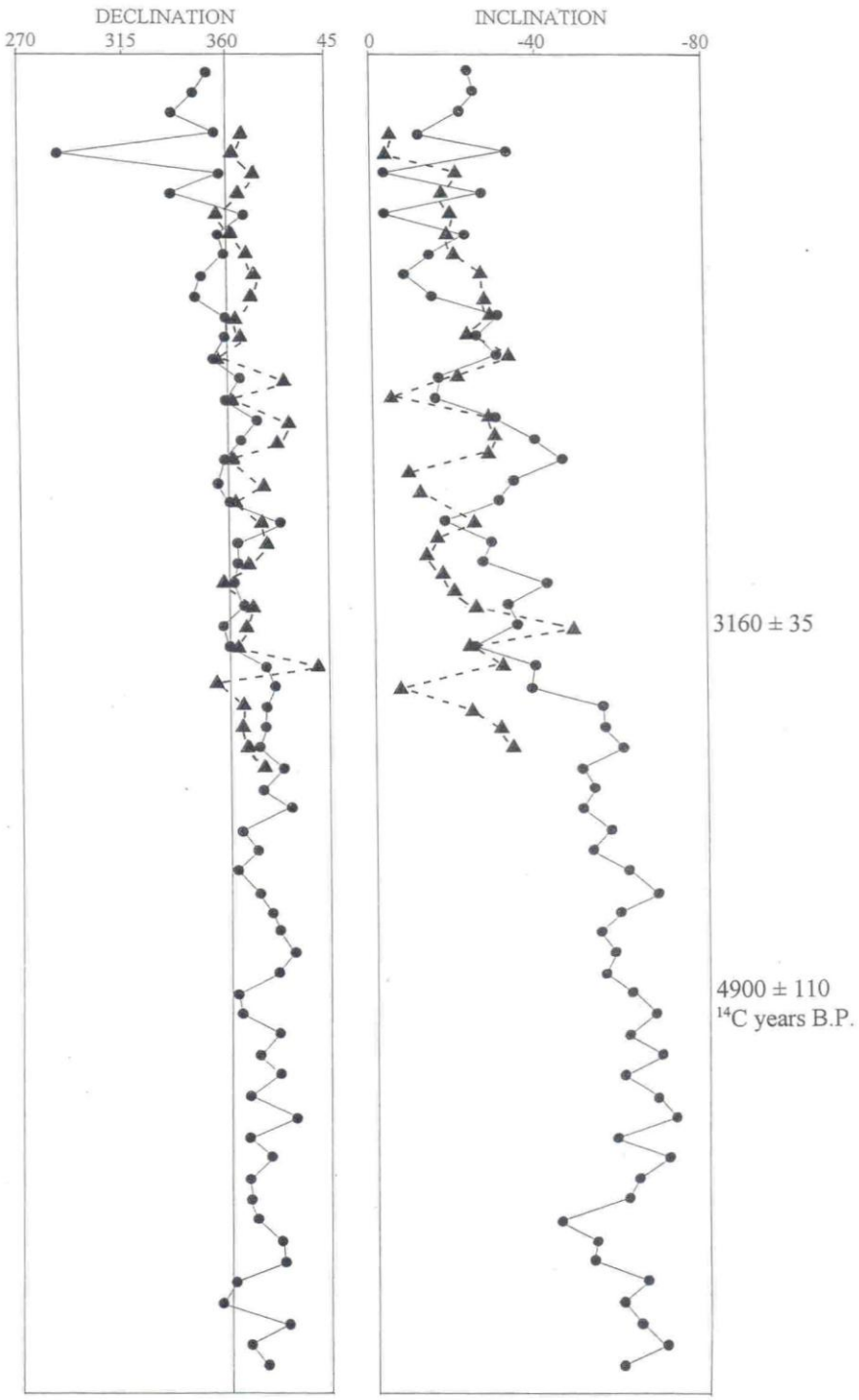

Figure 20. Overlapped presentation of the mean declination and inclination from the sites located in NE Corrientes province (showed in figure 17) and LM related with direct absolute dates by 14C. Triangle and dashed lines represents SL, BP and SJ sites, solid circles and continuous line illustrates LM.

Figura 20. Presentación superpuesta de la declinación e inclinación media de los sitios ubicados en el NE de la provincia de Corrientes (mostrado en la figura 17) y LM relacionadas con fechas absolutas de 14C directas. Los triángulos y líneas de trazos representan los sitios SL, BP y SJ. Los círculos y las líneas continuas ilustran a LM.

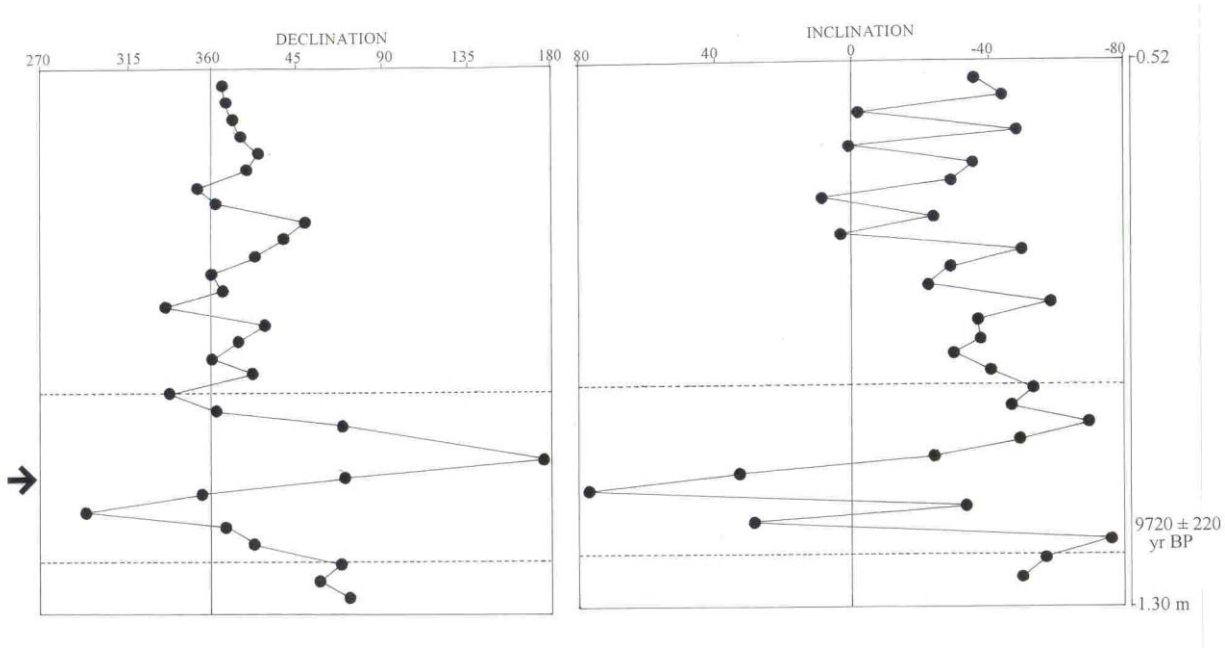

Figure 21. Declination and Inclination profile from SB2. The more conspicuous directions departures are depicted between dashed lines and pointed with an arrow.

Figura 21. Perfil de declinación e inclinación de SB2. Las direcciones con apartamientos más conspicuos se muestran entre las líneas punteadas y se señalan con la flecha.

Figure 23 depicts the virtual geomagnetic pole positions (VGP) calculated from the directions of the sites reported here. When plotted on a present world map, they show intermediate and reverse VGPs from the rotation axis of the Earth (Fig. 24). Those ones in the southern hemisphere are located in South America, South Africa, Australia and Antarctica. As illustrated in figure 25, these positions agree remarkably well with VGPs observed in previous paleomagnetic studies performed on Latest Pleistocene and Holocene sections from Argentina and Chile (Nami, 1999a; 2005). Remarkably is that this distribution shows strong similarities with the VGPs calculated for the Laschamp and Iceland basin excursions respectively dated at ~40 kya and ~180–220 kya interval (Laj and Channel, 2007: Fig. 5 y 8).

DISCUSSION AND CONCLUSIONS

New data obtained in sediments from different environments and lithologies cored along eastern Argentina have been found to contain records of anomalous GF behavior showing normal and intermediate polarity directions. In addition, there are several (ASE, PS, SB2 and CS) which also recorded reverse directions far from the present GF, probably corresponding to different field excursions occurred during the last ~11 kybp.

One of the most important geomagnetic polarity periods is the Brunhes Chron. This period corresponds to the last 780,000 years during which the GF polarity has been ‘normal’. However, there have been a number of occasions when the GF either briefly reversed or behaved anomalously. In other words, this normal polarity has been interrupted by significant departures from the dipole field configuration (Tarling, 1983; Lund et al., 2001). These kinds of departures are considerably larger than those seen in secular variations observed during historical times, and sometimes even attain opposite polarity, originating GF excursions. By definition, they are short intervals of locally anomalous field directions that occur within a broader interval of 'stable' normal or reversed magnetic polarity. GF directions have equivalent VGPs more than 45° away from the geographic pole during normal or reverse polarity (Watkins, 1976; Verosub and Banerjee, 1977). However, while certain excursions are known to be global, other ones, may have continental scale. During the last ~11 kybp several anomalous records with intermediate and reverse VGPs were observed at different materials, times and places. At ~2.0/2.5 kya the Starno event (Nöel and Tarling, 1975; Nöel 1975, 1977), the Etrussia excursion (Petrova and Pospelova, 1975; 1990; Raspopov et. al, 2003; Dergachev et al., 2004), the Sterno-Etrussia (Raspopov et al., 2003; Guskova et al., 2008) and Tahiti sea cores (Lund et al., 2007). Large amplitude fluctuations with reverse and intermediate polarities were also observed ~≤4-5 ky in lava flows and lacustrine sediments in Mexico (Gonzalez et al., 1997; Urrutia-Fucugauchi et al., 1995), Chinese fresh-water sediments from Beijing (Zhu et al., 1998) and the Red Rock site, California, USA (Nami, 1999b). Also, several cores from the Barents

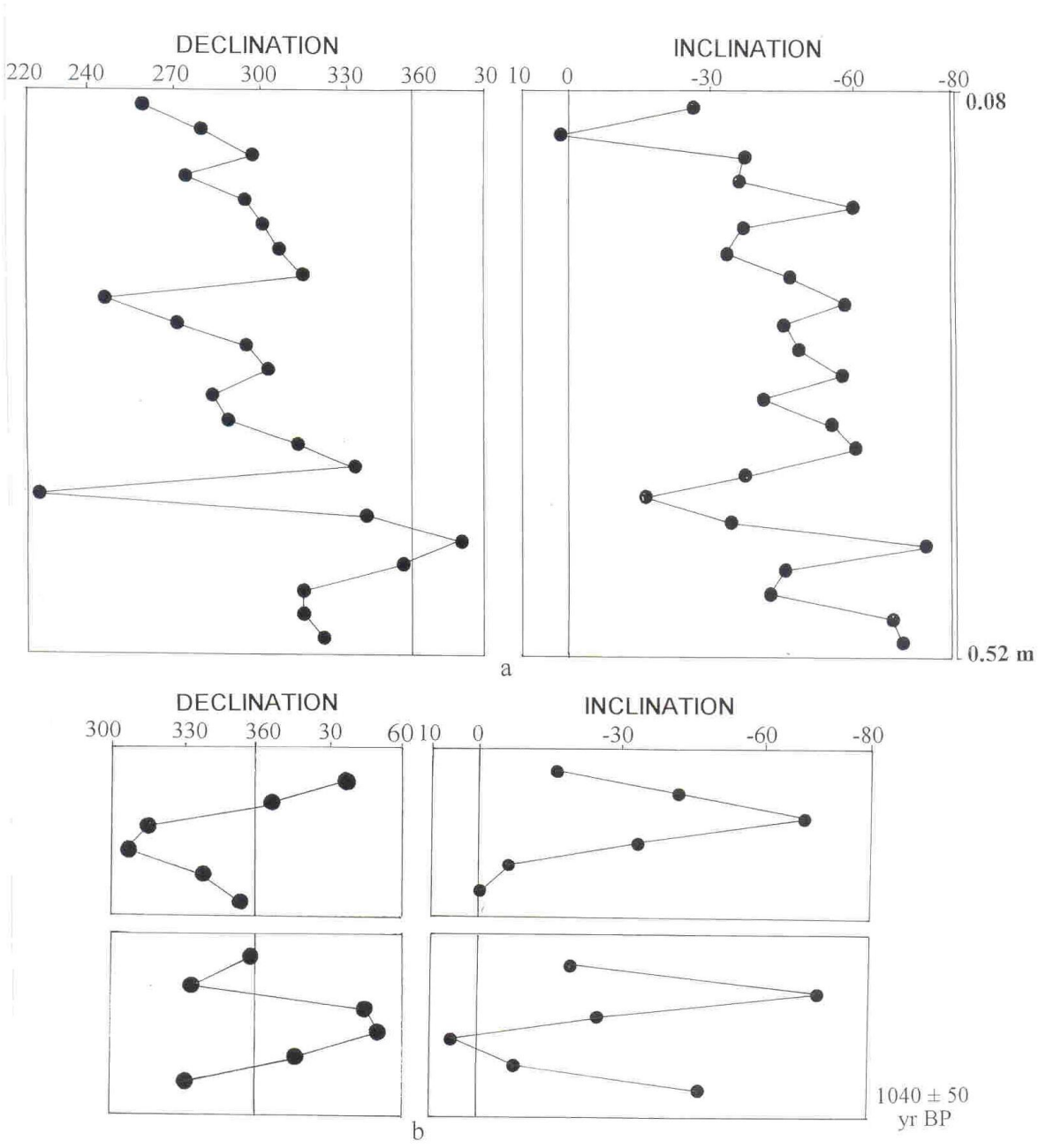

Figure 22. Declination and inclination logs according to their stratigraphic presentation from LMo (a) and CM (b).
Figura 22. Registros de declinación e inclinación según su presentación estratigráfica de LMo (a) y CM (b).

sea sediments yielded records of the Solovki excursion dated at 4.5-7.5 kya (Guskova et al., 2008). During the terminal Pleistocene and Holocene other anomalous directions were observed in a number of several sites and localities, such as the Erieau Lake (Creer et al., 1976), sea cores (Wiegank et al., 1990; Lund et al., 2007; 2008; Nelson et al., 2009) and El Tingo site in Ecuador (Nami, in prep.). As seen in table 1, they were also recorded in the Southern Cone of South America in sections that showed anomalous intermediate and reverse directions that remarkably agree with the above mentioned chronologies.

Then, during at least the last ~11-10 ky in some areas of the southern cone of South America, the GF might have been undergoing an anomalous behavior with large amplitude fluctuations, occasionally reaching reverse polarity positions, more than once. If they do represent the GF record, they are revealing that these kinds of directions might happen in a very short time span, probably decades or centuries; mainly during the terminal Pleistocene and early Holocene (~11-9/7 kya), middle (~5-4 kya) and late (~2.5-2.0 kya) Holocene. Also, very low negative and positive inclination values occurred in the last millennia and centuries (SL, LM, and CS). As previously reported, these kind of anomalous records were also observed in several parts of the Earth. Hence, the hypothesis of the global excursional state of the Holocene GF with not coetaneous intermediate and reverse directions was proposed (Nami, 1999b).

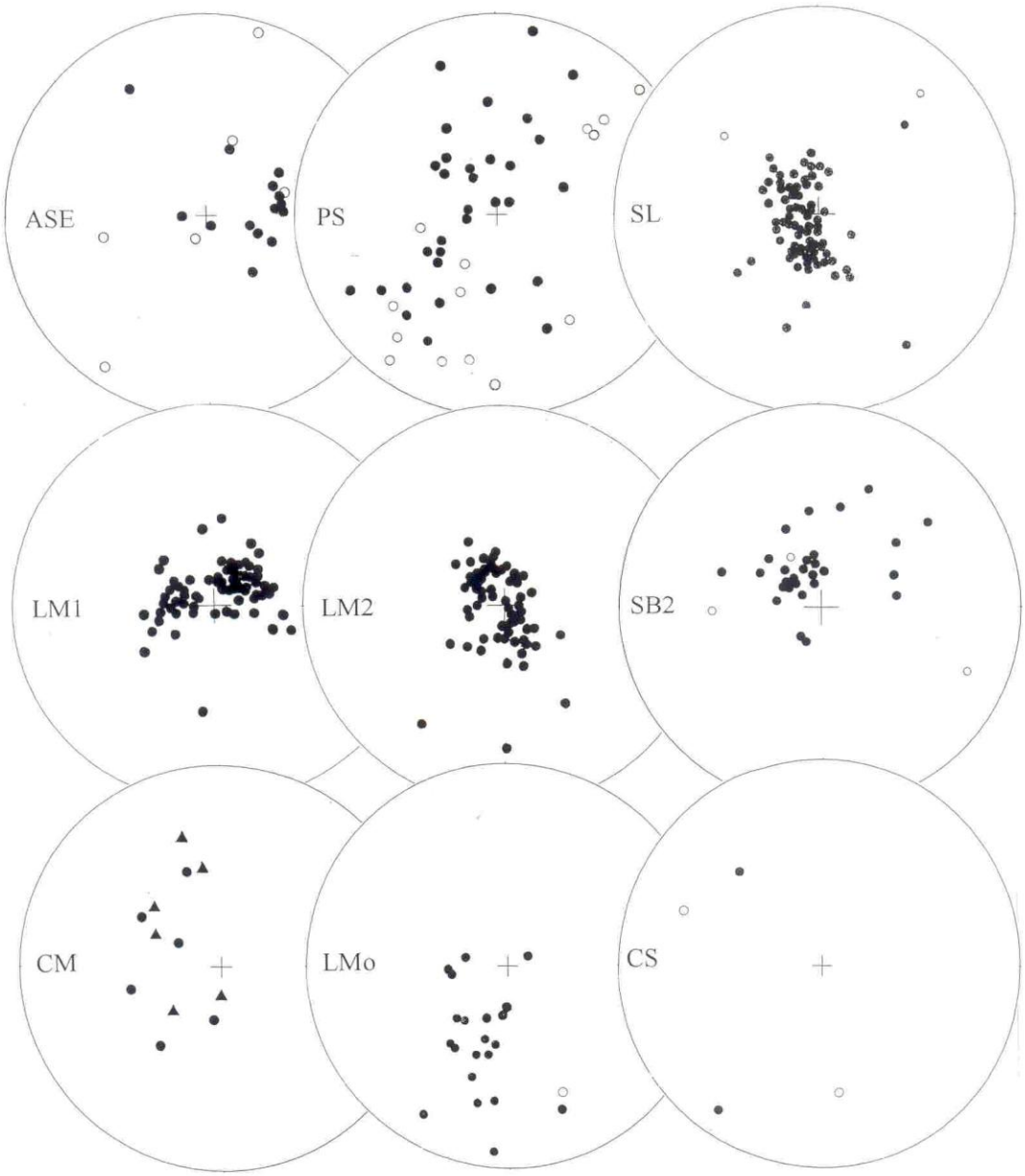

Figure 23. Stereographic projection of VGP calculated from directions of ChRM isolated in the sites mentioned in the text. Solid circles show those ones located in the Northern Hemisphere. The center of the projection is the Geographic Southern Pole.

Figure 23. Proyección esteoreográfica de PGV calculados de las direcciones de magnetizaciones remanentes características aisladas en los sitios mencionados en el texto. Los círculos llenos representan aquellos localizados en el Hemisferio Norte. El centro de la proyección es el Polo sur geográfico.

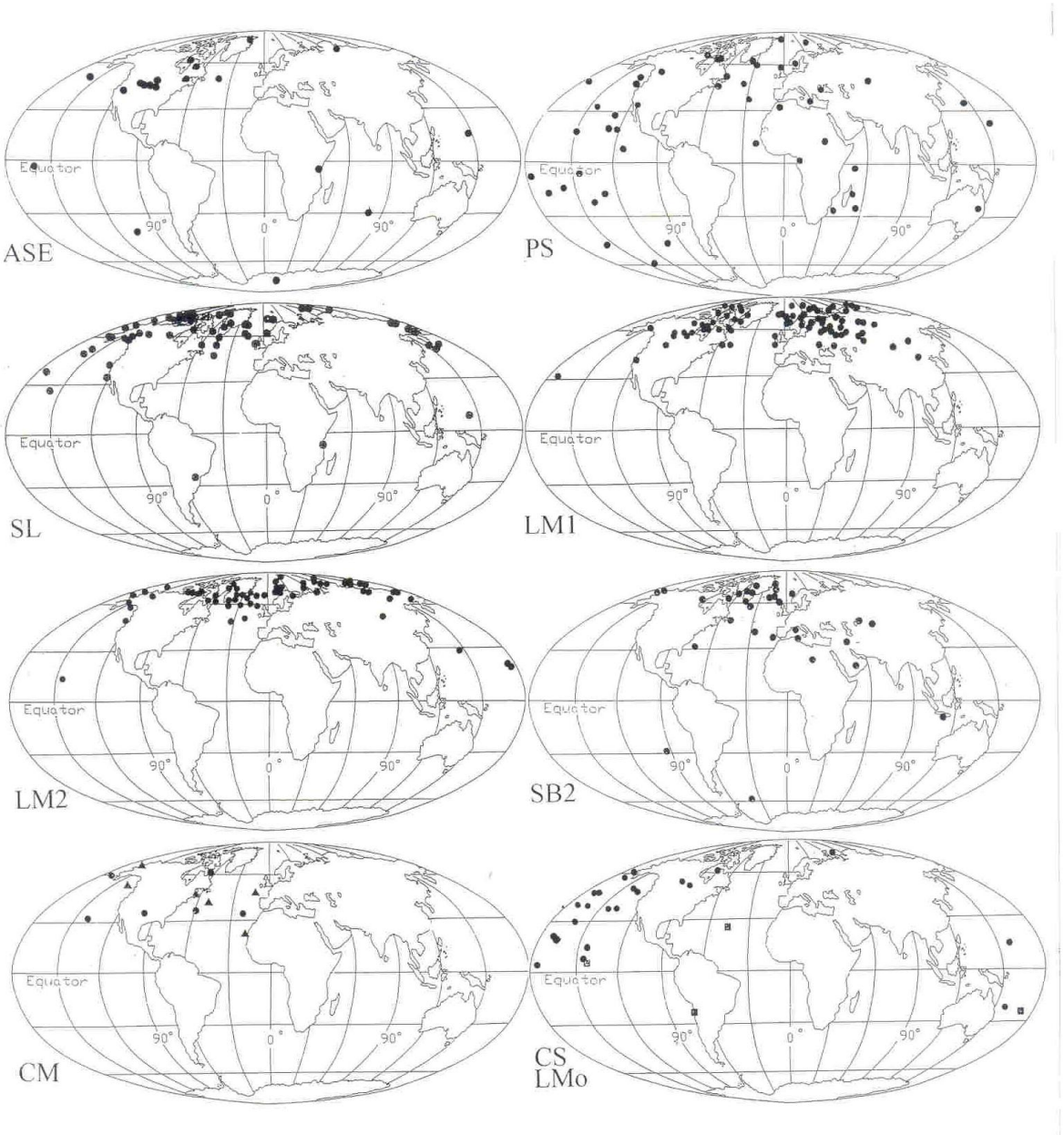

Figure 24. World map showing the location of the VGP obtained from the sites described in this paper.
Figura 24. Mapa del mundo mostrando la localización de PGV obtenidos de los sitios descriptos en este artículo.

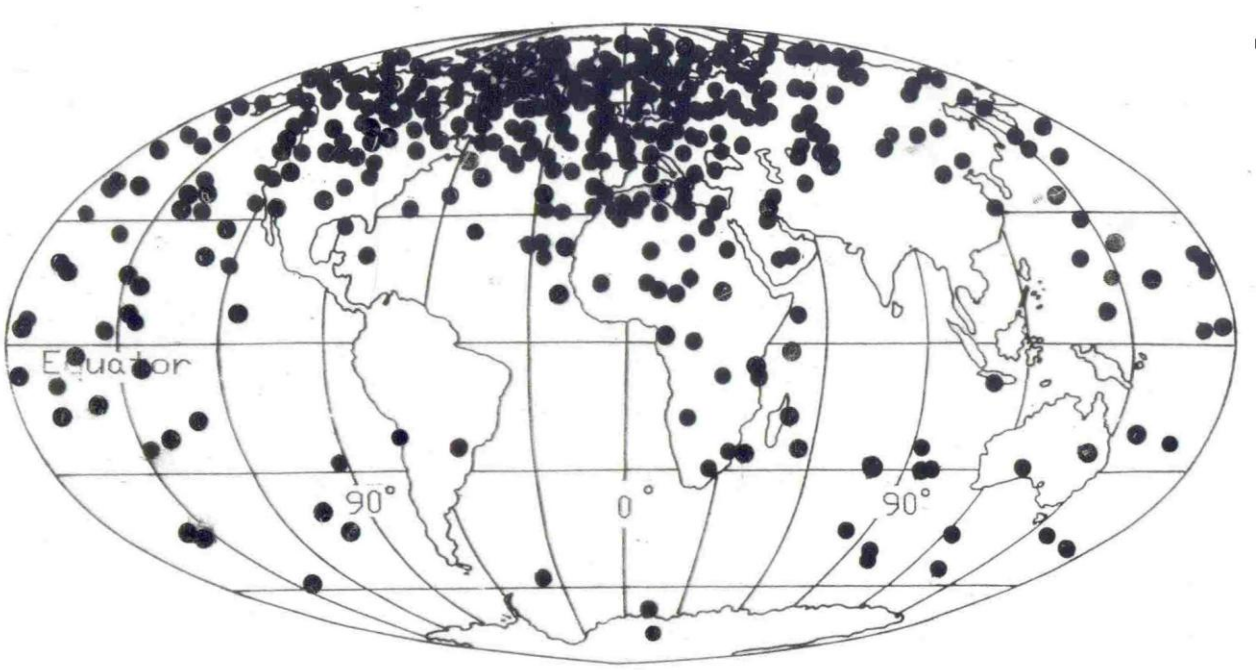

Figure 25. World map showing the location of the VGP calculated from the all sites with anomalous GM behavior located in the southern cone of South America.

Figura 25. Mapa del mundo mostrando la localización de PGV calculados de todos los sitios con conductas anómalas del campo geomagnético localizados en el cono sur de Sudamérica.

Site	Coordinates	Age (ky bp)	ND	P	N	SQ
Mylodon Cave	51° 35'S 72° 38'W	~11-5.5	31	N-R	34	HRe
Cueva del Medio	51° 35'S 72° 38'W	~11-2.1	20	N-I	12	MRe-Pre
Don Ariel	52°S 70° 09'W	~7-2.6	6	N-R	15	HRe-MRe
Las Buitreras	51° 45' S 70° 10´ W	≥10-4.3	2	N-I-R	40	HRe-MRe
Angostura Blanca	42° 30'S 70°W	~2.9-2.1	2	R-N	11	HRe-MRe-Pre
Alerode las Circunferencias	22° 56'S 65° 21'W	~10.7-7.9	5	N-I	36	HRe-MRe
Puerto Segundo	25° 59.03' S 54° 39.74' W	~7-0.6	*	I-R	50	HRe
Aserradero	26° S 54° 36.44' W	~7-1	*	N-I-R	20	HRe-MRe
Arroyo Yarará	26°S 55° W	~7-1	*	N-I	14	HRe-MRe
Barranca Pelada	30° 15'S 57° 37' W	~3.2-0.3	*	N-I	34	HRe-MRe
San Juan	30°S 57° 44' W	≥3.0	*	N-I	21	HRe-MRe
Santa Lucía	30° 15.7' S 57° 37.30' W	~11-0.2	1	N-I	74	HRe-MRe
Lomas del Mirador	34° 39.29' S 58° 32.17 W	~10-0.05	14	N-I	149	HRe-MRe
San Blas 2	40° 33.39' S. 62° 14.35 W	~9.6-≤5	1	N-I-R	30	HRe-MRe
Laguna Montecarlo	51° 55' S, 69° 39´ W	≤ 10	*	N-I	23	HRe-MRe
Cueva Montecarlo	51° 54.86' S 69° 38.79' W	~1	1	N-I	12	HRe-MRe
Cueva Saenz	51° 44.46'S 70°09.92' W	≤ 10	*	I-R	5	HRe-MRe

Table 1. Summary of number of sites, location, number and range of ^{14}C dates of sampled deposits, number, quality and polarity of the samples. References: ND: number of ^{14}C dates in the sites, *: indicate indirect dates, N: number of samples used in the analysis, P: polarity of the core, N: normal, I: Intermediate, R: reverse. Intemediate considered when departure from the mean is greater than 30° (Quideller and Vallet, 1996), HRe: highly reliable, MRe: moderately reliable, PRe: poorly reliable (Nami, 1999a).

According to Opdyke and Mejia (2004: 319) the study of the time averaged field shows that the GF is more variable that expected. This instability and its decrease in intensity may indicate that the GF is in process of becoming unstable leading to an excursion or reversal. Likely, the observations presented in this paper might be part of this instability process. Actually, in southern South America there is presently a zone of geomagnetic anomaly in the South Atlantic (Bloxham and Gubbins, 1985; Bloxham, 1995) and, according to Gubbins (1987, 1994) beneath the Atlantic Ocean there is a “reverse flux” patch. If the records presented here are not sediment artifacts (Langereis et al., 1992) and, considering that during the Holocene the GF was probably in excursional state, it might have a non-dipolar behavior (Bogue and Merril, 1992; Bogue and Paul, 1993). Then, it is expected that the Holocene GF might have had normal, intermediate and/or reverse polarity positions at the same time in different regions. Therefore, a possible interpretation is that the records presented here are a regional expression of the anomalous GF behavior with highly fluctuating records that has prevailed during Late Pleistocene/Holocene in eastern Argentina.

Several authors (Thouveny and Creer, 1992; Laj and Channel, 2007; Valet, 2008) state that as an anomalous GF behavior, a geomagnetic excursion is an event of large amplitude that occurred during a brief time span. As a significant GF anomaly, it often involves declines in field strength of between 0-20 % of normal (Lin et al., 1994; Fuller, 2006). Muscheler and colleagues (2000), pointed out that this kind of GF changes as well in the carbon cycle can produce variations in atmospheric radiocarbon (^{14}C) concentrations through the rate of ^{14}C removal from the atmosphere or, to variations in the production rate of ^{14}C due to changes in solar activity. These alterations might have had some implications in climate variability (Dergachev et al., 2004a; Kuznetsov and Kuznetsova, 2006; Kuznetsova and Kuznetsov, 2008; Usoskin and Kovaltsov, 2008). By virtue of the data presented in previous sections, as seen in figure 26 the reverse and intermediate directions observed in dated records from different parts of the world and the southern cone, agrees with the peaks of major fluctuations occurred in the curve proposed by Vonmos and colleagues (2006) that show the solar modulation function Φ based on the ^{14}C production rate (Stuiver and Braziunas, 1988) compared with the normal GF record for the past 11,450 years (Yang et al., 2000). On the other hand, the arrows in figure 27 shows the peaks indicating the changes in the GF behavior modulated the ^{14}C level and, the intensity of galactic cosmic rays intrusion into the Earth's atmosphere. Remarkably, some of them agree with the coldest conditions during the last 10 kya (Dergachev and Chistyakov, 2004b) and different GF excursions recorded during the Pleistocene/Holocene transition and Holocene. Finally, figure 28 illustrate that remarkably, the strongest fluctuations in radiocarbon series in time during the last 8 ky, occurred at 500, 2700, 5400 and 7200 years BP (Vasiliev and Dergachev, 2002) at similar times that the GF behaves anomalously during the Holocene.

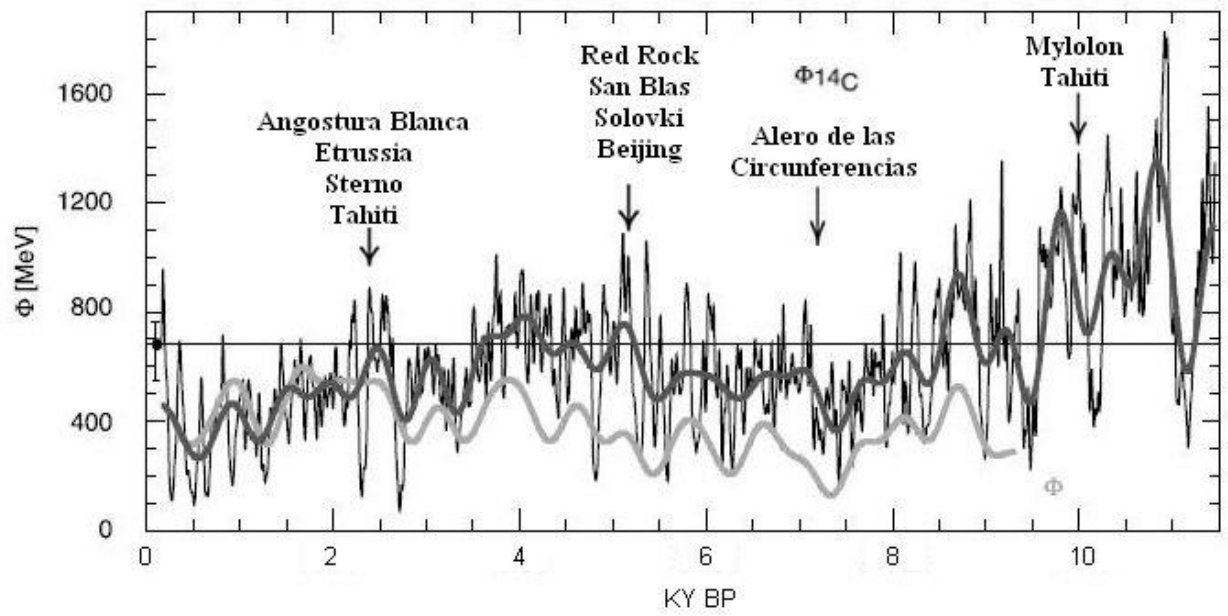

Figure 26. Records of dated excursions during the Pleistocene/Holocene transition and Holocene observed around the world related with peaks of major fluctuations occurred in the curve of solar activity record in terms of the solar modulation function Φ based on the 14C production and the geomagnetic field record for the past ~11.5 kya (Slightly modified after Vonmos et al. 2006: Fig. 6).

Figura 26. Registros de excursiones fechadas de la transición Pleistoceno/Holoceno y Holoceno mundialmente observadas relacionadas con los picos de las mayores fluctuaciones en la curva de actividad solar en función del índice de la producción de 14C y las excursiones del campo geomagnético de los últimos ~11.5 kya (Levemente modificado Vonmos et al. 2006: Fig. 6).

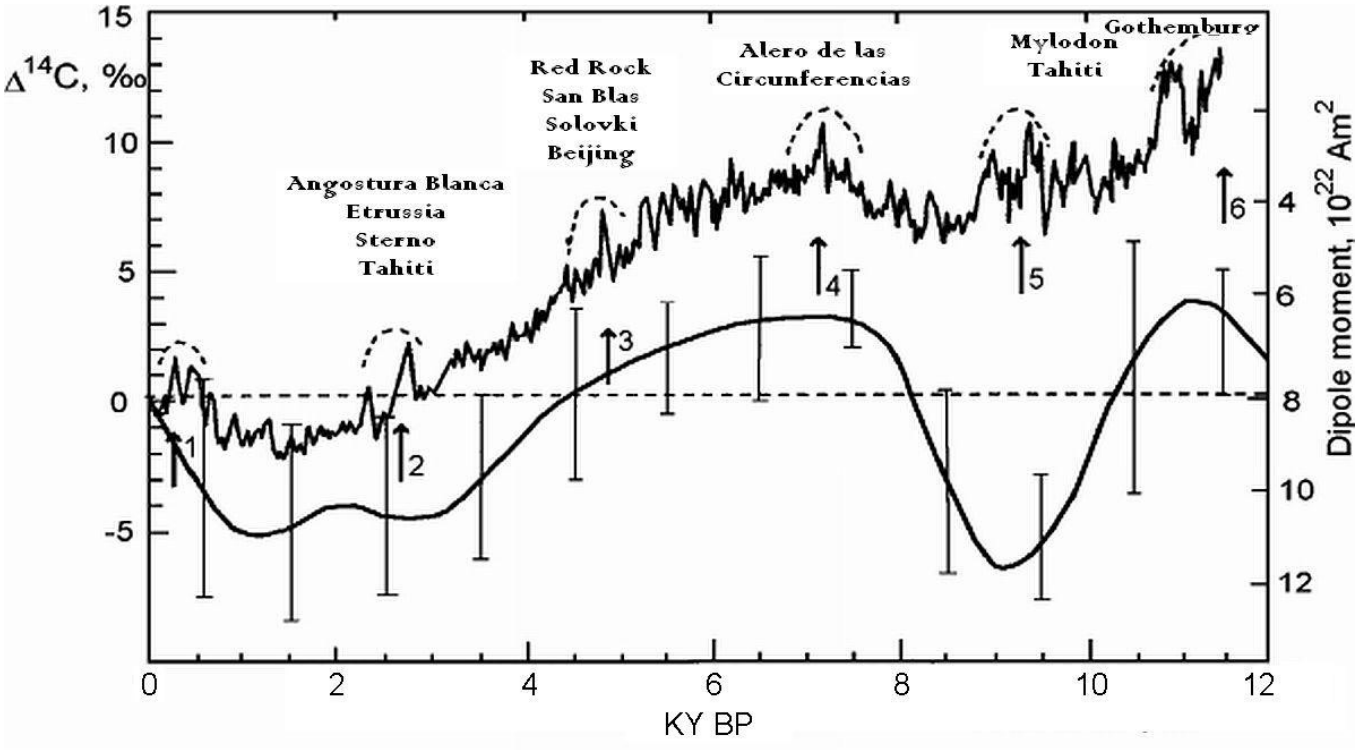

Figure 27. Changes in the normal GF behavior modulated the ^{14}C level and, the intensity of galactic cosmic rays. and different GF excursions recorded during the Pleistocene/Holocene transition and Holocene. The arrows shows the peaks of the galactic cosmic rays intrusion into the Earth's atmosphere (modified after *Dergachev et al.* 2004b).

Figura 27. Cambios en la conducta del campo geomagnético normal, el nivel modulado de ^{14}C y la intensidad de rayos cósmicos galácticos relacionados con las diferentes excursiones del campo geomagnético registradas durante la transición Pleistoceno/Holoceno y Holoceno. Las flechas indican los picos de intrusión de rayos cósmicos galácticos en la atmósfera de la Tierra (modificado de *Dergachev et al.* 2004b).

Acknowledgements: I am indebted to: M. Cuadrado Woroszylo, D. Curzio, J. Mujica, M. Silveira, J. and A. Gherardi were very helpful during the fieldwork and palaeomagnetic sampling; the University of Buenos Aires and CONICET for their support; J. L. Sáenz, A. Manero and G. Clifton for his friendship, continuous support and help in Río Gallegos, A. C. Sanguinetti de Bórmida was very supportive during the sampling in the northern Patagonian project (PMT-PICT0458). AMS dating was kindly provided by the NSF and IAI program for Latin American Quaternary research to global change studies. AMS measurement and age calculation was performed by the NOSAMS facility at Woods Hole Oceanographic Institute and the CU-Boulder INSTAAR Laboratory for AMS Radiocarbon; all other preparation of the samples was performed by the CU-Boulder INSTAAR Laboratory for AMS Radiocarbon Preparation and Research (University of Colorado at Boulder). Jocelyn Turnbull was very helpful during the AMS date processing. Several aspects of this research was supported by Agencia de Promoción Científica y Tecnológica, CONICET; National Geographic Society (Grant 5691-96); Logistic support during the fieldwork was provided by Secretaría de Cultura de la provincia de Misiones, Museo Regional "Juan P. Molina", Secretaría de Deportes de Santa Cruz, INTA and FOMICRUZ S.A. from Santa Cruz, Municipalidad de Monte Caseros; Ariztizábal family for allowing to work in his Estancia at the Chico river. Paleomagnetic data were processed with IAPD and MAG88 programs developed by Torsvik (Norwegian Geological Survey) and E. Oviedo (University of Buenos Aires) respectively. Especially to H. Vizán for his useful comments and stimulating feedback. Additional thanks to all the fellows at the Institute for their fruitful discussion and invaluable help during this research.

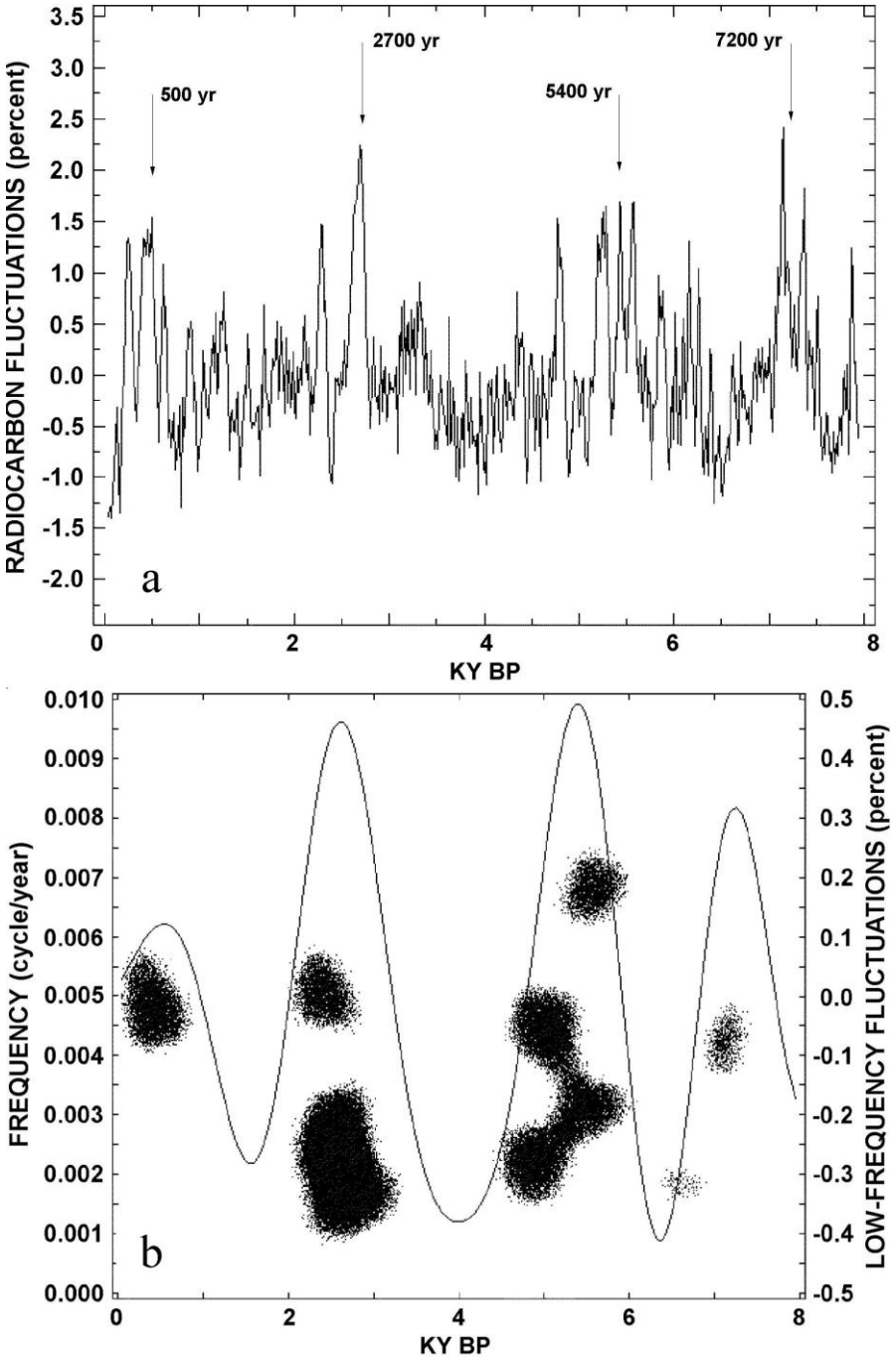

Figure 28. a) Radiocarbon series Δ14C D in time after long-term detrending. The strongest fluctuations occurred at 500, 2700, 5400 and 7200 years BP (before present). B) The domains of high amplitude (dark areas) on the frequency-time plane found in the radiocarbon data by the multiple filtration method. The epochs of fluctuations with high amplitude are repeated each 2300–2500 years. The cyclic curve is the result of low frequency filtration with maximum frequency 0.00066 cycle/year (Modified after Vasiliev and Dergachev 2002: Figs. 1 and 2).

Figura 28. a) Serie radiocarbónica Δ14C D en el tiempo según tendencias a largo plazo. Las fluctuaciones más fuertes ocurren a 500, 2700, 5400 and 7200 años BP. B). Dominios de alta amplitud (areas negras) sobre la el plano tiempo-frecuencia encontrado en los datos radiocarbónicos y el método de filtración múltiple. Las épocas de mayores fluctuaciones con alta amplitud se repiten cada 2300-2500 años. La curva cíclica es el resultado de filtraciones de baja frecuencia con frecuencia máxima 0.00066 año/ciclo (Modificado de Vasiliev y Dergachev 2002: Figs. 1 y 2).

REFERENCES

Bird, J., 1988. *Travels and Archaeology in South Chile*.Hyslop, J (Ed.), Iowa Univesity Press. Iowa.246 pp.

Bloxham, J., 1995. Global Magnetic Field. In: *Global Earth Physic. A Handbook of Physical Constants*, AGU Reference Shelf 1, American Geophysical Union, Washington D. C. 47-65.

Bloxham, J. and P. Gubbins, 1985. The secular variations of Earth's magnetic field. *Nature* 317: 777-781.

Bogue, S. W. and R. T. Merrill. 1992. The Character of the Field during Geomagnetic Reversals. *Annu. Rev. Earth Sci*. 20: 181-219.

Bogue, S. W. and H. A. Paul, 1993. Distinctive Field Behavior Following Geomagnetic Reversal. *Gephys. Res. Lett.* 20: 2399-2402.

Castellanos, A., 1975. Cuenca Potamográfica del Río de la Plata. In Geografía de la República Argentina. Hidrografía*.,* VII, 2° parte, Sociedad Argentina de Estudios Geográficos, Buenos Aires. 1-159.

Creer, K. M., Anderson, T. W. and C.F.M. Lewis, 1976. Late Quaternary geomagnetic stratigraphy recorded in the Lake Erieu sediments. *Earth and Planet. Sci. Lett*. 31: 37-49.

Creer, K. M., P. Tucholka, D. A. Valencio, A. M. Sinito, and J. F. Vilas, 1983. Results from Argentina. In: *Geomagnetism and Baked Clays and Recent Sediments*, Creer, K. M., P.Tucholka and C. E. Barton (Eds.), Elsevier, Amsterdan. 231-236.

Dawson, A. G., 1992. *Ice Age Earth. Late quaternary Geology and Climate.* Routledge, New York. 340 pp.

Dergachev, V. A., O. M. Raspopov, B. van Geel and G. I. Zaitseva, 2004a. The ´Sterno-Etrussia´ Geomagnetic Excursion around 2700 BP and Changes of Solar Activity, Cosmic Ray Intensity, and Climate. *Radiocarbon* 46: 661-681.

Dergachev, V. A., P. B. Dmitriev, O. M. Raspopov, and B. Van Geel, 2004b. The effects of galactic cosmic rays, modulated by solar terrestrial magnetic fields, on the climate. *Russ. J. Earth Sci.* 6 (5): 323-338.

Dunlop, D. J. and Ö. Özdemir, 1997. *Rock Magnetism. Fundamental and frontiers*. Cambridge University Press, Cambridge. 596 pp.

Fisher, R. A., 1953. Dispersion on a sphere. *Proc. R Soc. Ser. A.*, 217: 295-305.

Frink, D. S., 1992. The Chemical variability of carbonized organic matter through time. *Arch. E. N. Am.* 20: 67-79.

Frink, D. S., 1994. The oxidizable carbon ration (OCR): A proposed solution to some of the problems encountered with radiocarbon data. *N. Am. Arch.* 15 (1): 17-29.

Frink, D. S., 1995. Application of the Oxidizable Carbon Ratio Dating Procedure and its Implications for Pedogenic Research. In *Pedological Perspectives in Archeological Research,* Soil Science Society of America, Special Publication 44, Madison. 95-106.

Fuller, M., 2006. Geomagentic field intensity, excursions, reversals and the 41,000-yr obliquity signal. Earth Planet. Sci. Lett. 245: 605-615.

Gogorza, C. S. G., I. Di Tommaso, A. M. Sinito, B. Jackson, H. Nuñez, K. Creer and J. F., Vilas, 1998. Preliminary results from paleomagnetic records on lake sediments from South America. *Studia Geophys. Geod.* 42: 12-29.

Gogorza, C. S. G., A. M. Sinito, J. F. Vilas, K. Creer and H. Nuñez, 2000. Geomagnetic secular variations over the last 6500 years as recorded by sediments from the lakes of south Argentina. *Geophys. J. Int.* 143: 787-798.

Gonzalez, S., G. Sherwood, H. Bohnel and E. Schnepp, 1997. Palaeosecular variation in central Mexico over the last 30000 years: the record from lavas. *Geophys. J. Int.* 130: 201-219.

Grondona, M. F., 1975. Pendiente del Océano Atlántico, in Geografía de la República Argentina. Hidrografía*.,* **VII**, 2° parte, Sociedad Argentina de Estudios Geográficos, Buenos Aires. 203-394.

Gubbins, D., 1987. Mechanism for geomagnetic polarity reversals, *Nature* 326: 167-169.

Gubbins, D., 1994. Geomagnetic polarity reversals: A connection with secular variation and core-mantle interaction? *Rev. Geophys.* 32(1), 61–83.

Guskova, E.G., O.M. Raspopov, A.L. Piskarev, V.A. Dergachev, 2008. Magnetism and Paleomagnetism of the Russian Arctic Marine Sediments. *Proceedings of the 7th International Conference "Problems of Geocosmos"*, St. Petersburg. 380-385.

Isla, F. I., 1989. Holocene Sea-Level Fluctuation in the Southern Hemisphere. *Quat. Sci. Rev.* 8: 359-368.

Kirschvink, J. L., 1980. The least-squares line and plane and the analysis of palaeomagnetic data, *Geophys. J. R. astr. Soc.,* 62: 699-718.

Kuznetsov, V.V. and N.D. Kuznetsova, 2006. The Earth Palaeoclimate Response to Cosmic Rays Exposure During Geomagnetic Field Excursions *Proceedings of Geocosmos*, St. Petesburg. 112-115.

Kuznetsova, N. D. and V. V. Kuznetsov, 2008. Implications of Volcanism and Geomagnetic Field Polaritiy Reversals into the Climate Variability. *Proceedings of the 7th Conference "Problems of Geocosmos*", St. Petesburg. pp. 146-151.

Laj, C. and J. E. T. Channell, 2007. Gemagnetic Excursions*. Treatise Geophys*. 5V, Elsevier, Amsterdam. 373-416.

Langereis, C. G., van Hoof, A. A. M. and P. Rochette, 1992. Longitudinal confinement of geomagnetic reversal paths as a possible sedimentary artefact. *Nature* 358: 228-230.

Lin, J. L., Versoub, K. L. and A. P. Roberts, 1994. Decay of the virtual dipole moment during polarity transitions and geomagnetic excursions. *Geophys. Res. Lett.* 21: 525-528.

Lund, S.P., T. Williams, G. D. Acton, B. Clement and M. Okada, 2001. Brunhes Chron Magnetic Field Excursions Recovered from Leg 172 Sediments. In: *Proceedings of the Ocean Drilling Program, Scientific Results*. Keigwin, L.D., Rio, D., Acton, G.D. and Arnold, E. (Eds). 1-18.

Lund, S. P.. E. Platzman, N. Thouveny and G. Camoin, 2007. Evidence for Two New Paleomagnetic Field Excursions ~2,500 and ~12,500 Years Ago from the South Pacific Ocean Region (Tahiti). AGU, Fall Meeting, abstract #GP42A-05

Lund, S. P. E. Platzman, N. Thouveny, G. Camoin, Y. Yokoyama, H. Matsuzaki and C. Seard, 2008. Evidence for Two New Magnetic Field Excursions (11,000 and 13,000 Cal Yrs BP) from sediments of the Tahiti Coral Reef (Maraa tract). AGU, Fall Meeting, abstract #GP21B-0786

McElhinny, M. W. and P. L McFadden, 2000. *Paleomagnetism. Continents and Oceans*, Academic Press, Burlington, pp. 386.

Miller, E., 1987. Pesquisas arqueológicas paleoindígenas no Brasil occidental. *Est. Atacameños* 8: 37-61.

Muscheler, R., J. Beer, G. Wagner and R. C. Finkel, 2000. Changes in deep-water formation during the Younger Dryas event inferred from 10Be and 14C records. *Nature*: 408: 567-570.

Nami, H. G., 1994. Excursiones Geomagnéticas y Arqueología: Nuevos Datos y Perspectivas en la Patagonia. *Actas y Memorias del XI Congreso Nacional de Arqueología Argentina (Resúmenes). Rev. Mus. Hist. Nat. S. Rafael* XIII (1/4): 362-367.

Nami, H. G., 1995a. Holocene Geomagnetic Excursion at Mylodon Cave, Ultima Esperanza, Chile. *J. geomag. Geoelect.* 47: 1325-1332.

Nami, H. G., 1995b. Archaeological Research in the Argentinean Río Chico Basin. *Cur. Ant.* 36: 661-664.

Nami, H. G., 1999a. Possible Holocene Excursion of the Earth's Magnetic Field in Southern South America: New Records from Archaeological Sites in Argentina. *Earth Planets Space* 51: 175-191.

Nami, H. G., 1999b. Arqueología de la localidad arqueológica de Pali Aike, Cuenca del río Chico (provincia de Santa Cruz, Argentina). I. Las investigaciones arqueológicas. *Praehistoria* 3: 189-201.

Nami, H. G., 1999c. Probable middle Holocene geomagnetic excursion at the Red Rock archaeological site, California. *Geofís. Int.* 38: 239-250,

Nami, H. G., 2006. Preliminary paleomagnetic results of a terminal Pleistocene/Holocene record from northeastern Buenos Aires province (Argentina). *Geofizika* 23 (2): 119-141.

Nami, H. G. 2011. New detailed paleosecular variation record at Santa Lucía archaeological site (Corrientes province, northeastern Argentina). *Geofís. Int.* 50 (2): 9-21.

Nami, H. G. in prep. Detailed paleomagnetic record of the possible geomagnetic field excursion during the latest Pleistocene-early Holocene at el Tingo site, Ilalo valley, Ecuador.

Nami, H. G. and A. M. Sinito, 1991. Preliminary paleomagnetic results, the Campo Cerda Rockshelter, province of Chubut, Argentina. *Quat. South Am. Antarc. Penninsula* 9**:** 141-151.

Nami, H. G. and A. M. Sinito, 1993. Evidence of a Possible Excursion of the Geomagnetic Field Reistered During the Late Holocene in the Province of Chubut, Argentina. *Geoacta* 20: 19-26.

Nami, H. G. and A. M. Sinito, 1995. Primeros resultados de los estudios paleomagnéticos en sedimentos de Cueva del Medio (Ultima Esperanza, Chile). *Ans. Inst. Pat. S. Cs. H. 2*3**:** 135-142.

Nelson, F. E., G. S. Wilson and Shipboard party, 2009. Environmental magnetism and excursion record of the Pleistocene-Holocene transition in marine cores, West Coast South Island, New Zealand. *Geophys. Res. Abstacts* 11, EGU2009-430.

Nöel, M., 1975. The Paleomagnetism of varved clays from Blekinge, Southern Sweden. *Geologiska i Stockolm Förhanlingar* 97: 357-367.

Nöel, M., 1977. The Late Weichselian geomagnetic event. *Nature* 267: 181.

Nöel M. and D. Tarling, 1975. The Laschamp Geomagnetic Event. *Nature* 253: 705-707.

Opdyke, N. D. and V. Mejía. 2004. Earth´s Magnetic Field. In: *Timescales of the Paleomagnetic Field*. Channell, J. E. E., D. V. Kent, W. Lowrie and J. G. Meert (Eds.). Geophysical Monographs, 143, AGU, Washington D.C. 315-320.

Pessenda, L.C.R., S.E.M. Gouveia and R. Aravena, 2001. Radiocarbon Dating of Total Soil Organic Matter and Humin Fraction and its Comparison with 14C Ages of Fossil Charcoal*. Radiocarbon* 43 (2B): 595-601.

Petrova, G. N. and Pospelova, G. A., 1990. Excursions of the magnetic field during the Brunhes chron. *Phys.Earth Planet. Inter.* 63: 135-143.

Pirazzolli, P., 1996. *Sea-level changes in the last 20000 years.* John Wiley and Sons, Chichester, 211 pp

Quideller, J. and J. P. Vallet, 1996. Geomagnetic changes across the last reversal recorded in lava flows from La Palma, Canary Island. *J. Gophys. Res.* 101: 13,755-13,773.
Raspopov, O. M., V. A. Dergachev, E. G. Goos´kova, and N. A. Morner, 2003. Visual Evidence of the Sterno-Etrussia Geomagnetic Excursion (2700 BP)? *Geophys. Res. Abs.*, 5.
Rodriguez, J. and C. Cerutti, 1999. Las Tierras Bajas del Nordeste y Litoral mesopotámico. In: *Nueva Historia de la Nación Argentina* I: 109-122, Editorial Planeta, Buenos Aires.
Scharpenseel, H. W., 1971. Radiocarbon Dating of Soils-Problems, Troubles, Hopes. In: *Paleopedology. Origin, Nature and Dating*. Yaalon, D. H (Ed.). International Society of Soil Scientists and Israel University Press, Jerusalem. 77-88.
Schmitz, P. I., 1987. Prehistoric hunters and gatherers of Brazil. *J. World Preh.* 1:53–126.
Schnack, E. J., 1990. Cambios globales e impactos costeros: La región Atlántica de América del Sur. In: *Latinoamérica. Medio Ambiente y Desarrollo* De Felippi, R. (Comp.). Instituto de Estudios e Investigaciones del Medio Ambiente, Buenos Aires. 243-249.
Serrano, A., 1932. Exploraciones arqueológicas en el río Uruguay medio. Talleres gráficos Casa Predassi, Paraná. 89 pp.
Serrano, A., 1950. *Los primitivos habitantes de Entre Ríos*, Biblioteca entrerriana "General Perón", Ministerio de Educación, Paraná. 178 pp.
Sinito, A. M., Nami, H. G. and C. Gogorza, 1997. Analysis of Palaeomagnetic Results from Holocene Sediments Sampled at Archaeological Excavations in South America. *Quat. South Am. Antarc. Penninsula* 10: 31-44.
Sinito, A. M. and H. J. Nuñez, 1997. Paleosecular variations recorded on lake sediments from South America. *J. geomag. Geoelect.* 49: 473-483.
Sinito, A. M., C. Gogorza, H. G. Nami and M. A. Irurzun, 2001. Observaciones Paleomagnéticas en el Sitio Arqueológico Puesto Segundo (Misiones, Argentina). *Anales Asociación Física Argentina* 13: 237-241.
Smorczewski, M., 1994. Protocolo de análisis físico-químico, Laboratorio de Análisis de Suelo, INTA, MS.
Stein, J. K. 1992. Organic Matter in Arcaheological Contexts. In: *Soils in Archaeology* Holliday, V. T. (Ed.). Smithsonian Institution Press, Washington D. C. 193-216.
Stuiver, M. and T. F. Braziunas, 1988. The solar component of the atmospheric 14C record. In: *Secular Solar and Geomagnetic Variations in the Last 10,000 Years*, F. R. Stephenson and A. W. Wolfendale (Eds.), Springer, New York. 245– 266.
Sylwan, C. A. 1989. *Paleomagnetism, Paleoclimate and Chronology of Late Cenozoic Deposits in southern Argentina.* Department of Geology, Stockholm University, Stockholm. 110 pp.
Tarling, D., 1983. *Paleomagnetism*. New York, Chapman and Hall, pp. 379.
Trebino, L. G., 1987. Geomorfología y evolución de la costa en los alrededores del pueblo de San Blas, provincia de Buenos Aires. *Rev. Asoc. Geol. Arg.* XLII (1-2): 9-22.
Tonni, E. P., Cione, A. L.and A. J. Figini, 1999. Predominance of arid climates indicated by mammals in the pampas of Argentina during the Late Pleistocene and Holocene. *Palaeogeog. Palaeoclimatol. Palaecol*. 147: 257-281.
Thouveny, N. and K. M. Creer, 1992. Geomagnetic excursions in the past 60 ka: Ephemeral secular variation features. *Geology* 20: 399-402.
Urrutia-Fucugauchi, J., Lozano-García, S., Ortega-Guerrero, B. and M. Caballero-Miranda. 1995. Paleomagnetic and Paleoenvironmental studies in the southern basin of Mexico-II Last Pleistocene-Holocene Chalco lacustrine record. *Geofis. Int*. 34: 33-53.
Usoskin, I. G and G. A. Kovaltsov, 2008. Cosmic rays and climate of the Earth: Possible connection. *Comptes Rendus* Geoscience, pp. 441–450.
Valencio, D. A., Sinito, A. M., Creer, K. M., Mazzoni, M. M., Alonso M. S. and V. Markgraf, 1985. Paleomagnetism, sedimentology, radiocarbon age determinations and palynology of the Llao-Llao area, southwestern Argentina (lat. 41° S, long. 71° 30' W): Paleolimnological aspects. *Quat. South Am. Antarc. Penninsula* 3: 109-147.
Valet, J., 2008. Field Excursions and Reversals: Observational Constraints. American Geophysical Union, Spring Meeting, abstract #GP33A-03
Vasiliev, S. S. and V. A. Dergachev, 2002. The 2400-year cycle in atmospheric radiocarbon concentration: bispectrum of 14C data over the last 8000 years. *Annales Geophys.* 20: 115–120
Vázquez, C. A. and H. G. Nami, 2006. Mathematical model of ferromagnetic concentration grains applied to a fluvial Holocene soil from Buenos Aires Province (Argentina). *Earth Planets Space* 58: 1381-1387.
Verosub, K. and S.K. Banerjee, 1977. Geomagnetic excursions and their paleomagnetic record. *Rev. Geophys.* 15: 145-155.
Vonmoos, M., J. Beer, and R. Muscheler, 2006. Large variations in Holocene solar activity: Constraints from ^{10}Be in the Greenland Ice Core Project ice core. *J. Geophys. Res.* 111, A10105, doi:10.1029/2005JA011500.
Watkins N., 1976. Polarity group sets up guidelines. *Geotimes* 21: 18-20.

Wiegank, F., Petrova, G. N. and G. A. Pospelova, 1990. Magneto-Chronostratigraphic Scale Model, Brunhes Chron. Geomagnetic Field in Quaternary. Zipe 62: 169-177, Akademie der Wissnschafter der DDR, Postdam.

Yang, S., H. Odah and J. Shaw, 2000. Variations in the geomagnetic dipole moment over the last 12000 years. *Geophys. J. Int*. 140: 158–162.

Zhu, R. X., Coe, R. S. and X.X. Zhao, 1998. Sedimentary record of two geomagnetic excursions within the last 15,000 years in Beijing, China. *J. Geophys. Res.* 103 (B12): 30323-30334.

Zijderveld, J. D. A., 1967. AC demagnetization of rocks: Analysis of results. In: *Methods in Paleomagnetism*, D.W. Collinson, K. M. Creer, and S. K. Runcorn (Eds.), Elsevier, Amsterdam. 254–286.

Recibido: 23-5-2012
Aceptado: 22-8-2012